The Plant Cell, Vol. 19: 1145–1162, April 2007, www.plantcell.org © 2007 American Society of Plant Biologists

RESEARCH ARTICLES

Maize Histone Deacetylase *hda101* Is Involved in Plant Development, Gene Transcription, and Sequence-Specific Modulation of Histone Modification of Genes and Repeats [W]

Vincenzo Rossi,[a,1] Sabrina Locatelli,[a] Serena Varotto,[b] Guenter Donn,[c] Raul Pirona,[a] David A. Henderson,[d] Hans Hartings,[a] and Mario Motto[a]

[a] Consiglio per la Ricerca e Sperimentazione in Agricoltura, Istituto Sperimentale per la Cerealicoltura, Sezione di Bergamo, I-24126 Bergamo, Italy
[b] Dipartimento di Agronomia Ambientale e Produzioni Vegetali, Università di Padova, I-35020 Legnaro, Italy
[c] Bayer CropScience, D-65926 Frankfurt am Main, Germany
[d] Insightful Corporation, Seattle, Washington 98109-3044

Enzymes catalyzing histone acetylation and deacetylation contribute to the modulation of chromatin structure, thus playing an important role in regulating gene and genome activity. We showed that downregulation and overexpression of the maize (*Zea mays*) Rpd3-type *hda101* histone deacetylase gene induced morphological and developmental defects. Total levels of acetylated histones and histone acetylation of both repetitive and nonrepetitive sequences were affected in *hda101* transgenic mutants. However, only transcript levels of genes but not repeats were altered. In particular, *hda101* transgenic mutants showed differential expression of genes involved in vegetative-to-reproductive transition, such as *liguleless2* and *knotted*-like genes and their repressor *rough sheath2*, which are required for meristem initiation and maintenance. Perturbation of *hda101* expression also affected histone modifications other than acetylation, including histone H3 dimethylation at Lys-4 and Lys-9 and phosphorylation at Ser-10. Our results indicate that *hda101* affects gene transcription and provide evidence of its involvement in setting the histone code, thus mediating developmental programs. Possible functional differences between maize *hda101* and its *Arabidopsis thaliana* ortholog *HDA19* are discussed.

INTRODUCTION

Various levels of chromatin folding ensure the organization of DNA into a tightly packaged environment, which must be highly flexible to switch between repressive condensed to active accessible states. This dynamic property of chromatin can be mediated by enzymes that modify DNA and histones (Fischle et al., 2003). A variety of posttranslational modifications of histones has been identified, including acetylation, methylation, phosphorylation, ubiquitination, and others (Peterson and Laniel, 2004). It has been proposed that site-specific combinations of histone modifications, together with DNA methylation, correlate with distinct chromatin states and functions. This led to the concept of an epigenetic histone code, interpreted by cellular regulatory factors and inherited through mitosis and meiosis (Strahl and Allis, 2000; Margueron et al., 2005). Among different histone modifications, acetylation of N-terminal Lys residues correlates with transcriptional activation and is associated with other histone marks of gene activity (Dion et al., 2005; Pokholok et al., 2005; Schubeler and Turner, 2005). Furthermore, distinct patterns of Lys acetylation have been found to define functionally related groups of genes in fission yeast (*Saccharomyces cerevisiae*), suggesting gene-specific and combinatorial functions (Kurdistani et al., 2004). The enzymes responsible for the steady state of histone acetylation are histone acetyltransferases and histone deacetylases (HDACs). These enzymes are members of distinct gene families and exist as multiprotein complexes (Carrozza et al., 2003; Thiagalingam et al., 2003). They can be targeted to specific promoters through interaction with sequence-specific transcription factors to locally modify both histones and nonhistone proteins. They can also act globally to modulate the turnover of histone acetylation throughout the entire genome (Kurdistani and Grunstein, 2003).

Histone acetyltransferases, HDACs, and other factors involved in chromatin structure modulation are highly conserved in eukaryotes, including plants (Loidl, 2004). However, peculiarities of plant development and response to environmental cues result in marked differences, such as the presence of plant-specific HDACs and distinct regulatory mechanisms involved in the establishment and maintenance of epigenetic information. In the genome of different plant species, several potentially functional HDACs have been identified and classified into three distinct families: the Rpd3/Hda1 superfamily, the Sir2-related, and the plant-specific HD2-like HDACs (http://www.chromdb.org; Pandey

[1] To whom correspondence should be addressed. E-mail vincenzo.rossi@entecra.it; fax 39-035-316054.
The author responsible for distribution of materials integral to the findings presented in this article in accordance with the policy described in the Instructions for Authors (www.plantcell.org) is: Vincenzo Rossi (vincenzo.rossi@entecra.it).
[W] Online version contains Web-only data.
www.plantcell.org/cgi/doi/10.1105/tpc.106.042549

et al., 2002). The characterization of *Arabidopsis thaliana* HDAC mutants revealed that members of different classes and within the same group have evolved specific functions. For example, mutations of the Rpd3-type *HDA6* gene did not display apparent phenotypic alterations but affected transgenes and repetitive DNA silencing and the nuclear organization of *rDNA* loci (Aufsatz et al., 2002; Lippman et al., 2003; Probst et al., 2004). Conversely, mutations of *HDA19*, another Rpd3-related gene, displayed various developmental abnormalities associated with genome-wide changes in gene expression and suggest *HDA19* involvement in jasmonic acid and ethylene signaling of pathogen response (Tian and Chen, 2001; Tian et al., 2005; Zhou et al., 2005). It was also shown that *HDA19* is a component of the repressive system required to prevent root formation in the shoot pole during *Arabidopsis* embryogenesis (Long et al., 2006). Despite these findings, many aspects of the HDACs' involvement in plant development, as well as the mechanisms responsible for HDAC-mediated control of gene/genome activity, remain elusive. Furthermore, the HDACs' function in crop plants is poorly understood. Many crop plants, including maize (*Zea mays*), have a large genome with a complex organization due to the presence of high amounts of dispersed repetitive sequences (Messing et al., 2004). This results in a uniform genomic distribution of silencing-related epigenetic marks, which in *Arabidopsis* are mainly confined to microscopically well-defined constitutive heterochromatic regions (Houben et al., 2003). Similarly, species-specific patterns of histone acetylation during the cell cycle have also been reported (Jasencakova et al., 2001). These observations suggest that possible species-specific differences in the epigenetic regulation of genome activity, including HDAC function, might exist.

To date, 15 genes encoding putative HDACs have been identified in the maize genome (10 *Rpd3*/*Hda1*-, one *Sir2*-, and four *HD2-like* genes; http://www.chromdb.org), and members of all three HDAC families have been identified and biochemically characterized (Lusser et al., 2001), making maize one of the best-characterized systems for the study of these enzymes. Indications on the biological role of maize HDACs have emerged as Rpd3-type HDACs displayed differential expression during plant development, and they were shown to be physically associated with the maize retinoblastoma-related protein, a key regulator of cell cycle progression (Rossi et al., 2003; Varotto et al., 2003). The finding that overexpression of a rice (*Oryza sativa*) *Rpd3* gene leads to alterations in growth rate and plant architecture further supports the involvement of these enzymes in controlling cell division in cereals (Jang et al., 2003).

In this study, we report the functional characterization of a member of the maize Rpd3-type HDAC family, the *hda101* gene (according to Plant Chromatin Database indications and following the convention for maize nomenclature; previously named Zm *Rpd3I* or Zm *Rpd3/101*; Rossi et al., 1998; Varotto et al., 2003). Transgenic maize plants with specific up- and downregulation of *hda101* expression exhibited pleiotropic effects on plant development. Gene expression, including transcription of important regulators of meristem function and vegetative-to-reproductive transition, was affected. We found that total levels of di-acetylated histone H3 (H3ac) and tetra-acetylated histone H4 (H4ac) as well as histone acetylation in specific repeats and genes of the maize genome were altered in *hda101* mutants. Total and sequence-specific levels of histone H3 dimethylated at Lys-4 (H3K4me2, according to the new nomenclature proposed by Turner, 2005), dimethylated at Lys-9 (H3K9me2), and phosphorylated at Ser-10 (H3S10ph) were also affected. Furthermore, changes in the nuclear localization profile of H3K9me2 were observed in *hda101* mutants. Overall, these findings contribute to shed light on the role of *hda101* in modulating plant development, genome activity, and modification of histone marks.

RESULTS

Maize Plants with Upregulation and Downregulation of *hda101* Expression

To clarify the biological role of *hda101*, two experimental approaches were employed. First, we identified two lines with independent insertions of the *Mutator* (*Mu*) transposon within the 5′ transcribed untranslated region of the *hda101* gene. In these lines, however, the abundance of *hda101* transcript was not altered (data not shown). This may be due to *Mu* terminal regions-related promoter activity (Raizada et al., 2001) or, alternatively, to redundancy, since additional genes closely related to *hda101* may be present in the maize genome and indistinguishable in DNA gel blot analysis (see Supplemental Figure 1 online). In a second approach, transgenic mutant maize plants displaying up- and downregulation of *hda101* transcription were generated by transformation with plasmids that constitutively overexpressed (OE) *hda101* sense or antisense (AS) transcript, respectively (Figure 1A). Maize lines regenerated from callus cultures, but lacking plasmids used for transformation, were used as wild-type controls. A total of 21 OE and 33 AS independent T0 transformants were obtained. DNA gel blot analysis showed that these plants contained one to three independent insertions of the transgene within the genome (see Supplemental Figure 1 online). Seven OE and seven AS lines were selected for further studies, outcrossed to the B73 inbred line, and subsequently selfed to achieve plants homozygous for the presence of the transgene (see Methods for a description of the crossing scheme). RNA gel blot analysis displayed that all AS lines showed a reduced *hda101* mRNA level compared with the wild type, except for the AS39 line (Figure 1B, top left-hand panel); this downregulation correlated with the expression levels of the antisense transcript (Figure 1C, top panel). Conversely, two transcripts accumulated in OE compared with wild-type plants (Figure 1B, top right-hand panel). The hybridization of RNA gel blots with probes specific for the 5′- and 3′-ends of the *hda101* cDNA and with a probe recognizing the *nopaline synthase* (*nos*) polyadenylation region indicated that the two hybridizing mRNAs represent full-length *hda101* transcripts, one of which contains the *nos* termination and the other lacking this sequence (Figure 1C, middle panel). The perturbation of *hda101* expression was a transient effect, as wild-type levels of *hda101* mRNA were restored after transgene loss (Figure 1C, bottom panel). Hybridization of RNA gel blots with probes specific for additional members of the maize Rpd3 family, namely, *hda102* and *hda108*, showed that the amount of these transcripts was unaffected in OE and AS plants (Figure 1B), indicating that only *hda101* expression was specifically altered in these lines. Two polypeptides

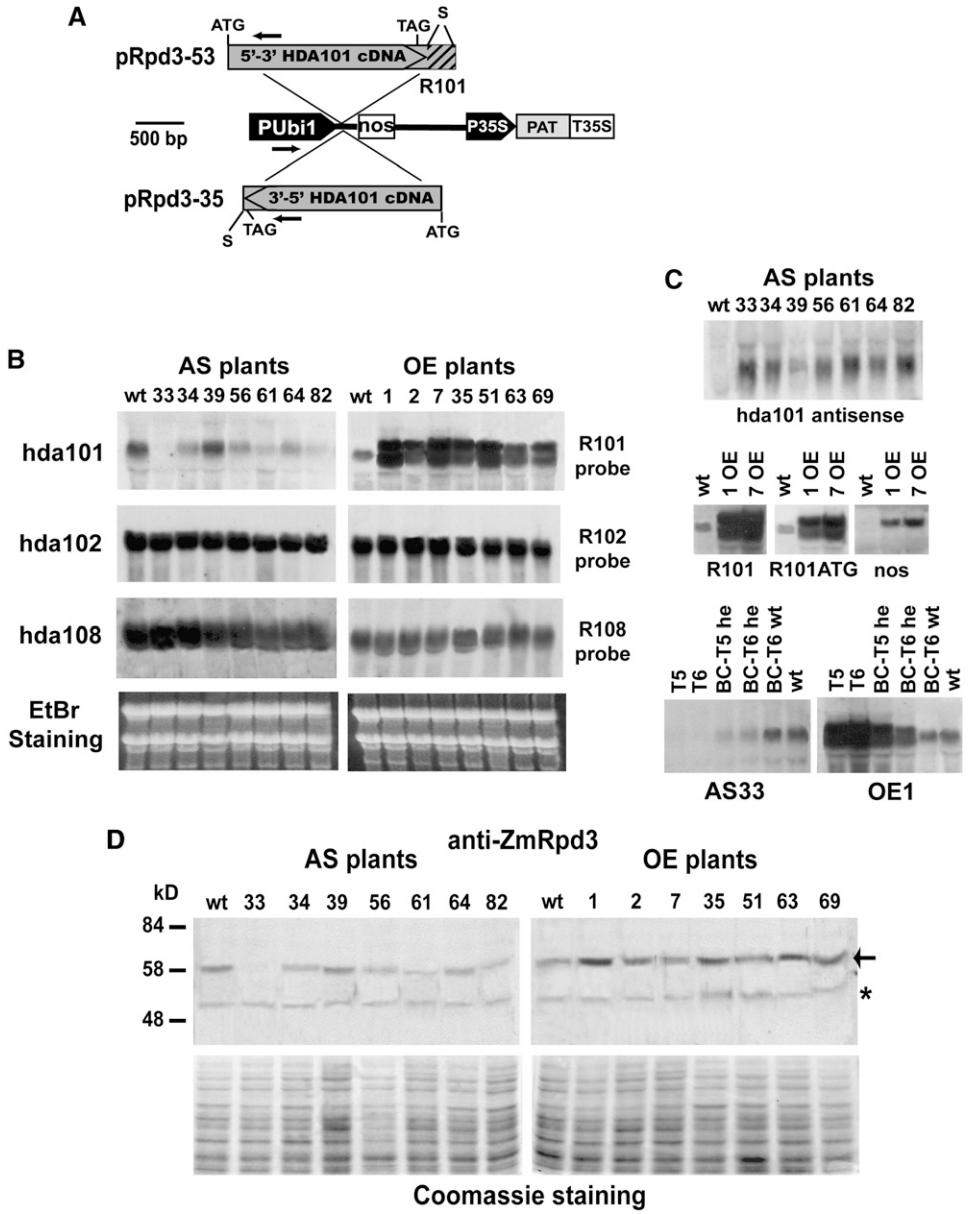

Figure 1. Upregulation and Downregulation of *hda101* Expression in Transgenic Maize Plants.

(A) Constructs containing *hda101* cDNA in sense (pRpd3-53) or antisense (pRpd3-35) orientation under the control of the constitutive Ubiquitin promoter (PUbi1) were used to transform maize protoplast and to obtain overexpressing (OE) and antisense (AS) *hda101* transgenic mutants, respectively. PAT, *phosphinothricin acetyl transferase* gene; P35S and T35S, promoter and 3′-region of the *Cauliflower mosaic virus*; nos, 3′ region of the *nopaline synthase* gene. Arrows mark the position of the primers used for PCR detection of the transgene. The hatched box represents the 3′-end region of *hda101* cDNA, which was deleted by *Spe*I (S) restriction in the pRpd3-35 antisense construct and was used as *hda101*-specific probe (R101 probe; see Methods for details) in RNA gel blots.

(B) Total RNA (20 μg per lane) extracted from T5 generation of AS, OE, and wild-type seedlings was fractionated through an agarose/formaldehyde denaturing gel, blotted, and hybridized with DNA probes (R101, R102, and R108) specific for the three members of the Zm *Rpd3* family (Varotto et al., 2003); RNA gel blots show *hda101*-specific increase/decrease of the mRNA level. Ethidium bromide staining of the gel is shown as input control.

(C) Hybridization with an *hda101*-specific DNA sense probe shows that each AS transformant expresses the antisense transcript (top panel). Hybridization with probes specific for 3′-end (R101) or ATG (R101ATG) *hda101* regions or for the nos polyadenylation region indicates that the two hybridizing mRNAs observed in OE transformants represent full-length *hda101* transcripts with different 3′-ends (middle panels). Transient effects on *hda101* up- and downregulation are observed in RNA gel blots (bottom panels) with RNA extracted from the wild type or from different generations of AS33 and OE1 seedlings: homozygous (T5-T6) or heterozygous (BC-T5 he and BC-T6 he) for the presence of the transgene or lacking the transgene due to plasmid segregation (BC-T6 wt; see Methods for details).

were detected in immunoblots with anti-ZmRpd3 antibody, the 58-kD HDA101 protein and a 51-kD polypeptide corresponding to HDA108 (Figure 1D; Varotto et al., 2003). The HDA108 protein level was similar in *hda101* mutants and the wild type. Conversely, alteration of HDA101 protein abundance correlated with differences in mRNA levels, although the variation of protein amount was less pronounced compared with changes in transcript levels. The slight differences in protein levels between transgenic lines might be due to cross-hybridization of the anti-ZmRpd3 antibody with additional members of the Rpd3 family. Up- and downregulation of *hda101* expression was also observed in immature maize seeds and inflorescences (data not shown).

Plants with Upregulation and Downregulation of *hda101* Expression Exhibit Phenotypic Alterations

Phenotypic analysis was performed on T5 and T6 progenies of homozygous transgenic mutants, revealing that perturbation of *hda101* expression induces several developmental defects. Seedlings of both AS and OE plants germinated normally; however, growth was slow during the vegetative phase (Figure 2A). Indeed, 2-week-old seedlings in five out of seven OE and five out of seven AS lines displayed a reduction of the first internode length, and the seedling dry weight in four OE and four AS lines decreased compared with the wild type (Table 1). This slow growth rate results in a delay of flowering and a reduction in adult plant height in most of the *hda101* transgenic mutants (Table 1, Figure 2B). The reduction of plant height was determined by shorter internodes because differences in the number of leaves were not observed. Adult *hda101* transgenic mutant plants showed additional developmental alterations. During field trials, an increase in the number of tillers was observed in five out of seven OE lines (Table 1). In particular, plants of the OE1 line showed a highly branched dwarf phenotype (Figure 2C). This phenotype is influenced by growing conditions because it was not observed when plants were grown in the greenhouse (cf. Figures 2B and 2C). Dissection of field-grown OE1 plants showed the formation of numerous basal, normally suppressed, axillary buds. Adult plants were highly tillered with long axillary branches developing from the majority of their nodes. Many of the tillers formed an apical inflorescence with pistillate and staminate florets that could produce pollen. Usually the inflorescences were formed by tassels that showed alteration in the placement of spikelet primordia and small regular ears; the tillers also produced regular and fertile ears (Figures 2D to 2F). Plants of the AS lines and particularly the AS33 line had curved leaves compared with wild-type plants (Figures 2G and 2H). Furthermore, inflorescence morphology and differentiation were affected in most AS and OE mutants. In four out of AS lines, tassel length was longer than in the wild type, while AS56 and four out of seven OE lines had a short tassel (Table 1). In both AS and OE plants, pollen shedding was limited due to abnormal anther dehiscence: anthers did not emerge at flowering and remained inside the glumes, although healthy pollen grains filled the anther locules (Figures 2I and 2K). Compared with wild-type plants, five out of seven OE mutants and the AS61 line produced numerous ears at the same and at different nodes (Table 1, Figures 2J and 2L). Fertility was usually partially reduced, and plants could set seeds after hand pollinations. In all OE and in four out of seven AS lines, a reduction of the kernel weight was observed (Table 1), and kernels and cobs were smaller at maturity (Figure 2M). Finally, the root dry weight of 2-week-old seedlings was reduced in four out of seven OE and in two out of seven AS lines, while the apical root was shorter in four out of seven OE and in four out of seven AS lines compared with the wild type (Table 1, Figure 2N). It is worth noting that a wild-type phenotype was restored when a transgene was removed by crossing to the wild-type recurrent parent.

These results indicate that the phenotypes described above were observed in multiple AS and OE lines. Therefore, one AS and one OE line were selected as representative of the two classes of the *hda101* transgenic mutants and used for subsequent molecular characterizations. In particular, we chose AS33 and OE1 lines since they displayed the most pronounced differences in *hda101* expression compared with the wild type (Figure 1) and exhibited most of the phenotypic alterations observed (Table 1).

Levels of Total Histone Acetylation and of Other Histone Modifications Are Altered in *hda101* Transgenic Mutants

Previous reports indicated that HDA101 exhibited HDAC activity (Lechner et al., 2000; Rossi et al., 2003). To ascertain whether alteration of *hda101* expression affects total levels of acetylated histones, we performed immunoblot analysis with histone extracts from transgenic and wild-type plants using antibodies specific for histones acetylated at different Lys residues. The global level of H3ac (di-acetylated at Lys-9 and Lys-14) and H4ac (tetra-acetylated at Lys-5, Lys-8, Lys-12, and Lys-16) was assessed in two AS (AS33 and AS61) and two OE (OE1 and OE63) lines. AS plants showed increased H3ac and H4ac levels, while their amount decreased in the OE plants with respect to the wild type (Figure 3A). In addition, we observed that the acetylation level at all single Lys residues analyzed was altered in AS33 and OE1 lines, although to a different extent; in particular, the amount of H4K16ac was only slightly affected (Figure 3B). To test whether changes in histone acetylation were correlated with changes in other histone modifications, we performed immunoblots with antibodies specific for H3K4me2 and H3S10ph, which

Figure 1. (continued).

(D) Crude protein extracts (100 μg per lane) from T5 generation of AS, OE, and wild-type seedlings were fractionated by SDS-PAGE, blotted, and immunodetected with anti-ZmRpd3 antibody (top panels), showing a decrease (AS) or increase (OE) of the 58-kD HDA101 polypeptide (indicated by the arrow) compared with the wild type. The amount of HDA108 51-kD protein (indicated by an asterisk) is unaltered. Coomassie staining shows equal protein loading.

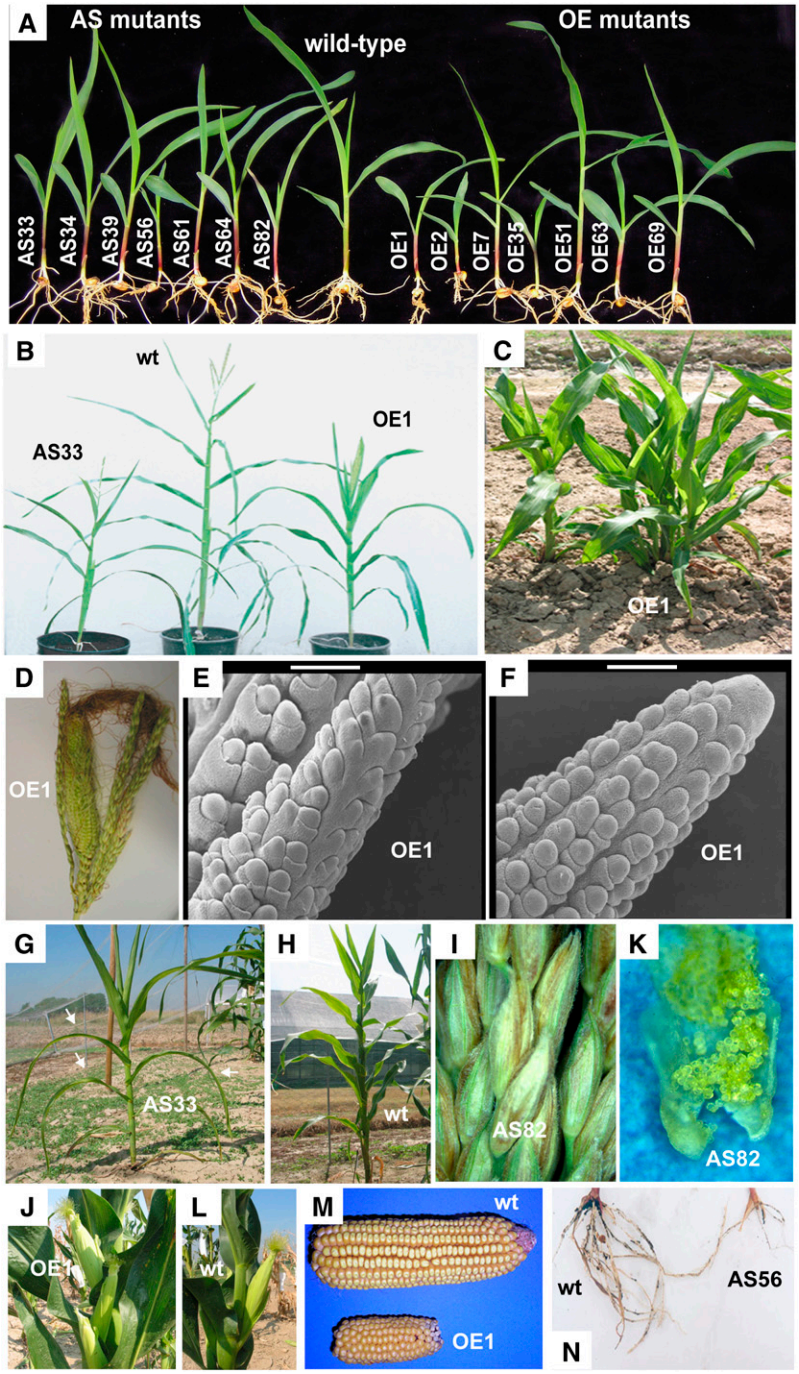

Figure 2. Perturbation of *hda101* Expression Induces Pleiotropic Effects on Plant Development.

(A) and **(B)** Greenhouse-grown T5 AS and OE plants display slower growth during vegetative phase **(A)**, resulting in reduced plant height compared with the wild type **(B)**.

(C) to **(N)** AS and OE mutants grown in field trials exhibit several morphological and developmental defects. A dwarf-branched phenotype is observed in OE lines and is particularly evident in OE1 plants **(C)**, which produce inflorescence from each tiller **(D)**. Electron microscopy scanning reveals that immature tassels of the tillers show differentiation of spikelet-pair primordia and alteration in the placement of spikelet primordia on the lateral branches **([E]**; bar = 200 μm), while tip of ear inflorescences exhibit characteristic sequence of development from spikelet-pair primordia to spikelet **([F]**; bar = 200 μm). AS 33 plants display limply appearing leaves (indicated by arrows in **[G]**) compared with wild-type plants **(H)**. Mutants exhibit defects in inflorescence development with anthers that remain inside glumes **(I)** but with locules that contain healthy pollen grains **(K)**. The production of numerous ears from the same or different node is observed in OE lines **(J)** compared with the one to two ears at different nodes observed in wild-type plants **(L)**. Both AS and OE lines generate smaller cobs and kernels **(M)**, and the seedlings display a reduction in the roots size and number **(N)**.

Table 1. Phenotypic Variations of AS and OE Lines

	Two-Leaf-Stage Seedlings[a]				Adult Plants[b]							
			Root Traits		Flowering Time		Plant Height					
	Seedling Dry Weight (mg)	First Internode Length (cm)	Root Dry Weight (mg)	Apical Root Length (cm)	Pollen Shed (GDD)	Silking (GDD)	Plant (cm)	Ear (cm)	Tassel Length (cm)	Ear Number	Tiller Number	100 Seeds Weight (g)
Wild type	187 ± 33	6.0 ± 1.1	110 ± 19	19.2 ± 5.9	842 ± 13	858 ± 23	186.6 ± 12.6	85.3 ± 11.2	36.3 ± 1.8	1.70 ± 0.63	0.35 ± 0.58	27.9 ± 1.4
OE1	60 ± 4	2.9 ± 0.7	32 ± 9	10.3 ± 4.1	967 ± 26	998 ± 32	134.7 ± 8.2	/	30.7 ± 2.5	4.05 ± 1.23	3.60 ± 1.54	16.5 ± 0.4
OE2	50 ± 17	2.7 ± 1.4	28 ± 3	8.4 ± 2.1	1010 ± 47	1051 ± 37	156.6 ± 15.0	/	29.6 ± 2.3	3.35 ± 1.08	1.05 ± 1.10	13.3 ± 0.3
OE7	70 ± 25	4.6 ± 1.1	39 ± 17	8.3 ± 2.7	/	/	122.6 ± 13.8	53.1 ± 12.1	29.1 ± 1.9	3.15 ± 1.09	1.10 ± 0.91	24.1 ± 0.2
OE35	49 ± 30	3.1 ± 1.5	27 ± 23	8.3 ± 5.4	889 ± 23	906 ± 16	157.1 ± 6.2	/	30.8 ± 2	2.60 ± 0.99	1.45 ± 1.15	19.8 ± 0.5
OE51	/	/	/	/	/	/	/	/	/	/	/	21.7 ± 0.3
OE63	/	5.1 ± 0.7	/	/	/	906 ± 22	160.3 ± 8.6	/	/	2.23 ± 0.71	0.95 ± 0.37	21.0 ± 0.6
OE69	/	/	/	/	/	/	/	/	/	/	/	23.3 ± 0.3
AS33	140 ± 23	5.2 ± 0.8	/	13.4 ± 5.4	931 ± 18	957 ± 16	149.8 ± 11.1	60.6 ± 8.2	39.3 ± 2.1	/	/	22.5 ± 1.0
AS34	/	5.0 ± 1.4	/	/	879 ± 15	887 ± 12	/	65.1 ± 7.0	40.3 ± 1.7	/	/	19.5 ± 0.2
AS39	/	/	/	/	/	/	/	/	/	/	/	/
AS56	64 ± 31	3.2 ± 1.7	30 ± 25	8.0 ± 4.3	1085 ± 43	1167 ± 48	94.3 ± 10.1	40.1 ± 5.9	29.3 ± 2.35	/	/	12.7 ± 0.5
AS61	142 ± 34	5.0 ± 1.3	/	13.0 ± 5.0	914 ± 31	943 ± 16	158.1 ± 11.0	66.2 ± 5.0	/	2.15 ± 0.88	/	/
AS64	/	/	/	/	884 ± 21	/	/	/	40.6 ± 2.8	/	/	/
AS82	33 ± 12	3.3 ± 0.8	12 ± 8	3.3 ± 2.4	987 ± 31	1048 ± 38	135.1 ± 15.0	44.0 ± 4.1	41.3 ± 2.5	/	/	15.8 ± 0.2

[a] Phenotypic traits were measured when the greenhouse-grown wild-type seedlings were at the two-leaf stage (2 weeks after sowing).

[b] Phenotypic traits were obtained during field trials when all the plants were at maturity. Mean and SE for each trait are reported.

The data were obtained using a minimum of 20 plants of the T5 progenies. Three samples of 100 seeds were used to measure weight. Similar changes in adult traits were observed in field trials using T6 progenies and in greenhouse-grown T5 plants. The flowering time is expressed in growing degree days (GDD). Plant and ear heights are measured from ground level to the base of the tassel and to the node bearing the uppermost ear, respectively. For clarity, only traits exhibiting statistically significant difference compared to the wild type by Student's *t* test analysis ($P < 0.01$) are shown. A slash indicates not significant changes.

are usually associated with gene activity (Fischle et al., 2003) and with an antibody specific for the heterochromatin marker H3K9me2. Results revealed that hyperacetylation in the AS33 line was accompanied by an increase in levels of H3K4me2 and H3S10ph, while opposite relationships were observed in the OE1 line (Figure 3C). The level of H3K9me2 was similar in mutants and the wild type. Immunoblots performed using histone extracts from homozygous and heterozygous AS33 and OE1 mutants revealed that the global levels of H3ac and H3K4me2 were altered only in the homozygous lines (Figure 3D). Furthermore, plants that had lost the transgene due to genetic segregation exhibited H3ac and H3K4me2 amounts similar to those observed in the wild type, indicating that reestablishment of a normal rate of *hda101* expression determines the reversion of both histone modifications to wild-type levels.

Nuclear Distribution of H3K9me2 Is Affected in *hda101* Transgenic Mutants

To determine whether the nuclear distribution of modified histones was affected in *hda101* transgenic mutants, interphase nuclei from AS33, OE1, and wild-type plants were stained with antibodies specific for modified histones and counterstained with 4′,6-diamidino-2-phenylindole (DAPI). DAPI staining distinguished the nucleolus, devoid of dye, and highly condensed chromatin regions that displayed intense labeling (Figure 4; see Supplemental Figure 2 online) and that have been identified as knobs (Shi and Dawe, 2006). The DAPI-stained nuclei of mutants were similar to the wild type. Results showed that, in *hda101* mutants, compared with the wild type, no marked variation of nuclear localization for H4ac, H3K4me2, and H3S10ph was detected (see Supplemental Figure 2 online). However, our resolution for detecting changes was limited by the widespread distribution of these histone marks and by the strong reduction of the signal intensity in OE1 nuclei, possibly due to a decrease of the global level of these histone modifications (Figure 3; see Supplemental Figure 2 online for details and for nuclear localization patterns exhibited by H4ac, H3K4me2, and H3S10ph). Changes in nuclear localization were instead evident for H3K9me2 (Figure 4). In wild-type nuclei, H3K9me2 was uniformly distributed along the whole chromatin, including densely DAPI-stained chromatin regions. In nuclei of *hda101* mutants, H3K9me2 was distributed less uniformly compared with the wild type. Indeed, in AS33 and OE1 nuclei, the signal intensity increased in correspondence to euchromatin and knobs, respectively.

Transcript Levels of Nonrepetitive Sequences, Including Regulators of Plant Development, but Not Repeats Are Altered in *hda101* Transgenic Mutants

To analyze whether *hda101* transgenic mutants affect expression of DNA sequences in the maize genome, the transcript levels of three categories of sequences were analyzed.

First, we used preliminary data from microarray analysis, performed using RNA extracted from 2-week-old wild-type, AS33, and OE1 seedlings as an initial screen to select sequences showing differential expression. The transcript levels of these sequences were then analyzed by real-time RT-PCR. A total of 27 sequences, representing all possible categories of expression changes in AS33 and OE1 versus wild-type lines, were selected.

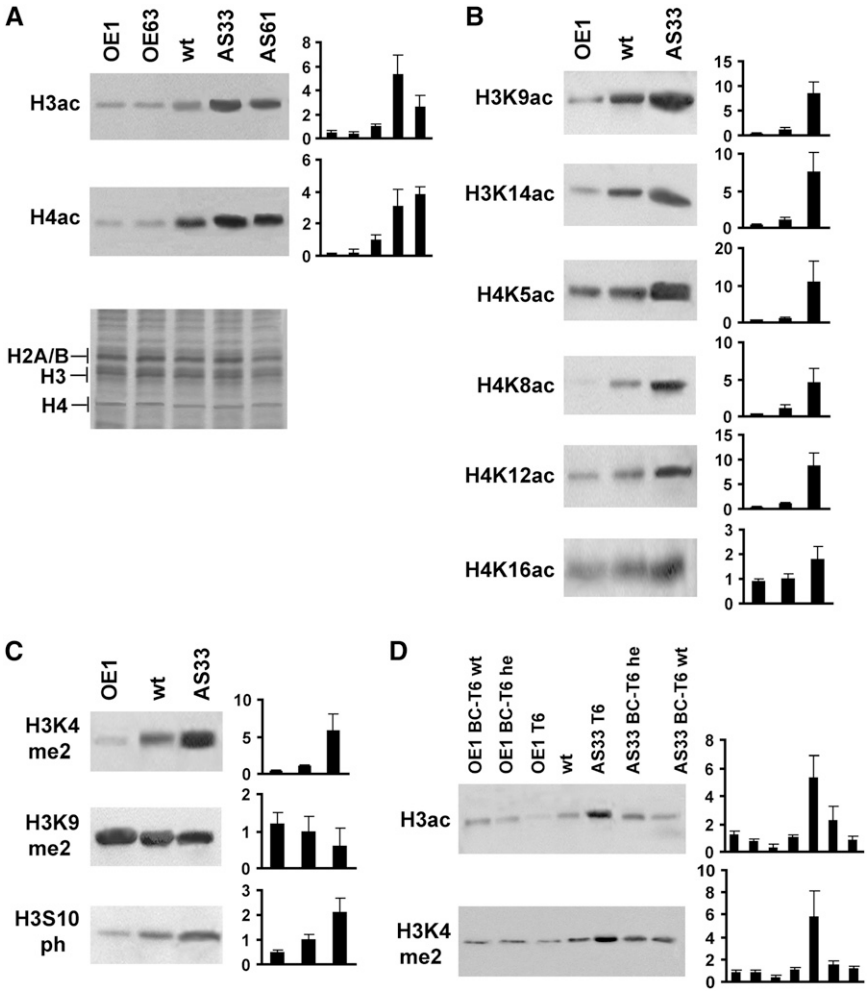

Figure 3. HDA101 Affects Total Levels of Modified Histones.

(A) to **(D)** Histone extracts from T5 generation of OE, AS, and wild-type plants were fractionated by 15% SDS-PAGE, blotted, and immunodetected using specific antibodies. All immunoblots were replicated at least twice. The hybridizing bands were quantified using Scion Image software; fold differences compared with the wild type and standard errors are reported in bar diagrams at the right of each panel.

(A) Total levels of acetylated histones were analyzed using antibodies recognizing H3ac and H4ac (left panels). A representative Coomassie staining of an SDS-PAGE gel is shown as loading control, and bands corresponding to maize histones are indicated.

(B) Antibodies specific for a series of single acetylated Lys residues in the N-terminal tails of histone H3 and H4 were employed to analyze histone extracts from OE1, AS33, and the wild type.

(C) Immunoblots were also performed using α-H3K4me2, α-H3K9me2, and α-H3S10ph antibodies.

(D) H3ac (top panel) and H3K4me2 (bottom panel) were further detected in OE1 and AS33 plants homozygous (T6) or heterozygous (BC-T6 he) for the presence of the transgene, from wild-type plants, and from plants that have lost the transgene following genetic segregation (BC-T6 wt).

According to changes in their expression profile, the 27 genes were grouped into nine classes. For example, genes with higher than wild-type expression in the AS33 line and lower than wild-type expression in the OE1 line were assigned to class A, genes with higher than wild-type expression in the AS33 line and expression equivalent to the wild type in the OE1 line were assigned to class B, etc. (Table 2). To distinguish between changes in gene expression induced by alteration of the HDA101 function and unrelated effects, such as transgene insertion and selectable marker expression, real-time RT-PCR analysis was conducted using RNA extracted from two AS and two OE lines. We used AS33 and AS61 *hda101* antisense and OE1 and OE63 *hda101* overexpressing lines, which displayed similar changes in global levels of H3ac and H4ac (Figure 3A). Results indicated that 16 out of the 27 selected sequences showed statistically significant changes of their transcript levels in the two AS or in the two OE lines compared with the wild type (Table 2). Two additional sequences, *gapc2*, encoding glyceraldehyde-3-phosphate dehydrogenase 2, and *ac1*, encoding actin 1, displayed no changes in their transcript levels and were enclosed in class H as

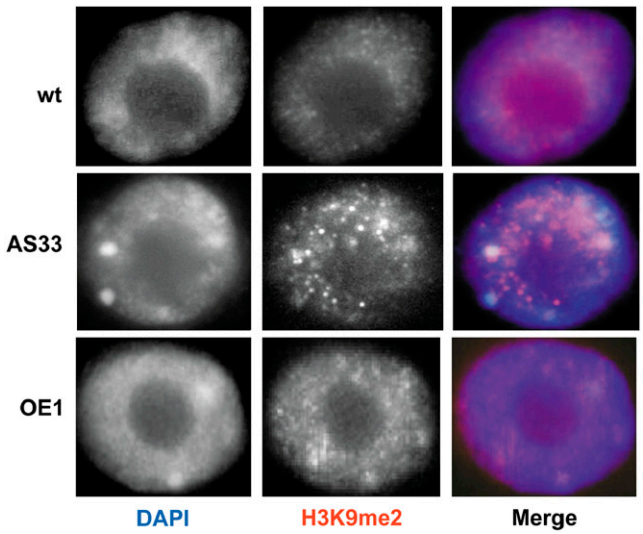

Figure 4. Effect of the Alteration of *hda101* Expression on Nuclear Distribution of H3K9me2.

Nuclei from wild-type, AS33, and OE1 plants were stained with DAPI (left panels) and immunostained (middle panels) with α-H3K9me2 antibody to detect distribution of this histone modification. Right panels show merged images. A minimum of 150 nuclei from mutants and wild-type lines was analyzed. Images are representative of the nuclear distribution patterns observed in at least 85% of the labeled and analyzed nuclei.

control genes. These results indicate that gene transcription was either positively or negatively affected in *hda101* transgenic mutants.

Expression of a second category of nonrepetitive sequences was also analyzed. Phenotypic analysis showed that *hda101* transgenic mutants had a slow growth rate and a delay in flowering time compared with wild-type plants, suggesting that *hda101* is involved in the control of plant development. Hence, the transcript levels of 10 genes encoding important regulators of plant development were evaluated by RT-PCR analysis. In particular, we assessed the expression of all cloned maize genes known to control the transition from juvenile-to-adult and from vegetative-to-reproductive phases. Genes investigated included *anther ear1*, *dwarf1* (*d1*), and *d3* (Evans and Poethig, 1995); *glossy15* (*gl15*; Moose and Sisco, 1994); *indeterminate1* (Colasanti et al., 1998), and *liguleless2* (*lg2*; Walsh and Freeling, 1999). Moreover, OE mutants displayed a dwarf phenotype and showed high proliferation of axillary meristems, recalling some morphological alterations observed in the *teosinte branched1* (*tb1*) mutant (Hubbard et al., 2002). Therefore, we analyzed the expression profile of the *tb1* gene and of homeobox genes required for meristem initiation and maintenance, including the *knotted*-like genes (Kerstetter et al., 1994) *knotted1* (*kn1*) and *rough sheath1* (*rs1*), and their repressor *rs2*, encoding a myb-domain protein (Timmermans et al., 1999; Tsiantis et al., 1999). All the 10 genes mentioned above, with the exception of *gl15*, are mainly or exclusively expressed in shoot meristems and/or tissues containing a high percentage of proliferating cells. Therefore, in addition to RNA extracted from 2-week-old seedlings, RNA prepared from 1.5- to 2-cm shoots harvested 5 to 7 d after sowing (hereafter named as 1-week-old shoots) was used for RT-PCR analysis, being the latter most suitable to detect variation in the expression profile of the selected genes. Results showed that in 2-week-old seedlings and 1-week-old shoots, the transcript level of the *lg2* gene increased in the two AS lines and decreased in the two OE lines compared with the wild type (Figure 5; data not shown). In addition, both *kn1* and *rs1* genes were expressed in 1-week-old OE shoots but not in AS and wild-type lines (Figure 5). A concomitant decrease of the *rs2* mRNA level was observed in the OE transgenic mutants. No expression of *kn1* and *rs1* was detected in 2-week-old seedlings of OE and wild-type lines, and no significant difference in the *rs2* transcript level was observed at this developmental stage (data not shown). The mRNA level of the other developmental genes analyzed herein did not reveal a statistically significant variation (F test; $P < 0.05$).

All sequences described above are nonrepetitive sequences, except one, the TC254543 sequence, which encodes a putative Tam3-like transposase and showed an increased expression in AS compared with wild-type and OE lines (Table 2). Therefore, we assessed whether the transcript levels of other repeats were altered in *hda101* transgenic mutants. Repeats analyzed include retroelements (*Cinful*, *Huck2*, and *Opie2*), *Mu* transposons (terminal inverted repeat and MuDRa transposase regions), centromeric repeats (CentC satellite, long terminal repeat, and gag regions of centromeric element of maize [*CRM2*]), and *rDNA* genes (*rDNA 5*, *rDNA 26S*, and intergenic spacer between *26S* and *18S* genes). Semiquantitative RT-PCR assays revealed that eight out of 12 repeats analyzed were expressed in wild-type seedlings, while the remaining failed to reveal a cDNA amplification product after 40 amplification cycles (Table 3; see Supplemental Figure 3 online). Real-time RT-PCR analysis indicated that, with the exception of the TC254543 sequence, none of the repeats analyzed exhibited differences in their transcript levels in the *hda101* transgenic mutants compared with the wild type (see Supplemental Figure 3 online).

Histone Acetylation of Repetitive and Nonrepetitive Sequences Is Affected in *hda101* Mutants

Histone modifications within specific repetitive and nonrepetitive sequences were analyzed using chromatin immunoprecipitation (ChIP) with antibodies against modified histones, followed by quantification of the immunoprecipitates by real-time PCR. It was shown that nucleosome density is not homogeneous across the genome and that HDAC subtypes can influence histone occupancy (Huebert and Bernstein, 2005; Wiren et al., 2005). This implies that nucleosome-rich and nucleosome-poor regions may appear as more and as less modified than they really are, respectively. Hence, we used an antibody against the histone H3 C-terminal region (H3 cter) to control for nucleosome occupancy. Results showed the importance to correct for nucleosome density in ChIP assays. Indeed, AS33 and OE1 transgenic mutants displayed a relative tendency to nucleosome loss and enrichment, respectively (see Supplemental Figure 4 online), thus affecting the number of sequences showing differences in the levels of modified histones between the wild type and mutants.

Table 2. Real-Time RT-PCR Quantification of Transcript Levels

Exp. Class	Sequence Accession/Name	AS versus Wild Type		OE versus Wild Type	
		AS33 versus Wild Type	AS61 versus Wild Type	OE1 versus Wild Type	OE63 versus Wild Type
A	TC313780*	1.66 ± 0.08	2.05 ± 0.03	−3.45 ± 0.12	−2.22 ± 0.16
AS33 and AS61 > wt	T18745*	1.62 ± 0.29	2.07 ± 0.29	−2.13 ± 0.20	−1.82 ± 0.03
OE1 and OE63 < wt	TC261045	1.74 ± 0.23	5.40 ± 1.68	−4.35±1.91	−7.14 ± 2.86
B	TC257813*	2.52 ± 0.25	1.87 ± 0.04	/	/
AS33 and AS61 > wt	TC254543 (repeat)*	5.53 ± 0.34	7.82 ± 2.03	/	/
OE1 and OE63 = wt	TC310872	2.64 ± 0.76	1.78 ± 0.35	/	/
C					
AS33 and AS61 > wt	TC271027	233.40 ± 40.93	977.76 ± 21.95	119.93 ± 37.24	26.61 ± 8.18
OE1 and OE63 > wt					
D					
AS33 and AS61 < wt	TC272335	−2.17 ± 0.46	−1.68 ± 0.20	1.75 ± 0.23	1.91 ± 0.33
OE1 and OE63 > wt					
E					
AS33 and AS61 < wt	BM073916	−2.43 ± 0.27	−2.63 ± 0.07	/	/
OE1 and OE63 = wt					
F	AZM4_15378	−3.85 ± 0.50	−4.55 ± 0.21	−1.69 ± 0.13	−4.65 ± 0.21
AS33 and AS61 < wt	TC248035	−166.5 ± 67.01	−2.18 ± 0.06	−5.56 ± 0.69	−10.31 ± 6.90
OE1 and OE63 < wt					
G					
AS33 and AS61 = wt	AI964645	/	/	2.66 ± 0.32	2.32 ± 0.51
OE1 and OE63 > wt					
H	*gapc2*	/	/	/	/
AS33 and AS61 = wt	*ac1*	/	/	/	/
OE1 and OE63 = wt					
I	TC249385	/	/	−2.63 ± 0.07	−1.85 ± 0.11
AS33 and AS61 = wt	TC251766*	/	/	−2.38 ± 0.11	−1.92 ± 0.16
OE1 and OE63 < wt	TC248146*	/	/	−91.00 ± 1.10	−1.82 ± 0.06
	TC287704	/	/	−5.00 ± 1.15	−2.17 ± 0.05

Experiments with maize arrays purchased from University of Arizona (http://www.maizearray.org) were employed to select sequences for subsequent real-time RT-PCR analysis, which was performed using two different cDNA preparations and at least three replicates for each preparation. Genes are grouped in nine different expression classes, according to changes in their expression profile in mutants versus the wild type (wt). Class H contains genes that do not exhibit alteration of expression. Results are expressed as the mean value and SE of the fold differences of mRNA level in AS or OE lines compared with the wild type. For clarity, only statistically significant differences (F test from analysis of variance [ANOVA]; $P < 0.05$) are reported, and a slash indicates no significant changes. An asterisk indicates sequences that showed changes in H3ac or H4ac level.

Comparison of chromatin immunoprecipitates and background signal, measured by omitting antibody during the ChIP procedure, revealed that most of the repeats analyzed exhibited a significant level of histone acetylation in wild-type seedlings (see Supplemental Figure 5 online). Downregulation of *hda101* expression in AS33 seedlings determined H3ac and/or H4ac enrichment in 10 out of the 12 repeats (Table 3). Conversely, *hda101* overexpression in OE1 seedlings induced hypoacetylation in five of these sequences. Therefore, the perturbation of *hda101* expression affects histone acetylation of repeats, although no alteration of their transcript levels was noted.

ChIP assays were further employed to assess histone acetylation within the coding region of the 27 previously analyzed nonrepetitive sequences (17 genes selected from microarrays and 10 developmental genes) and in the putative promoter region of 15 of these 27 genes, for which genomic sequences encompassing this domain were available. Results showed that the coding region of seven out of 27 genes and the putative promoter region of three out of 15 sequences exhibited differences in H3ac and/or H4ac levels between *hda101* transgenic mutants and the wild type (Table 4; see Supplemental Figure 6 online). Histone acetylation in the coding and promoter regions of all other

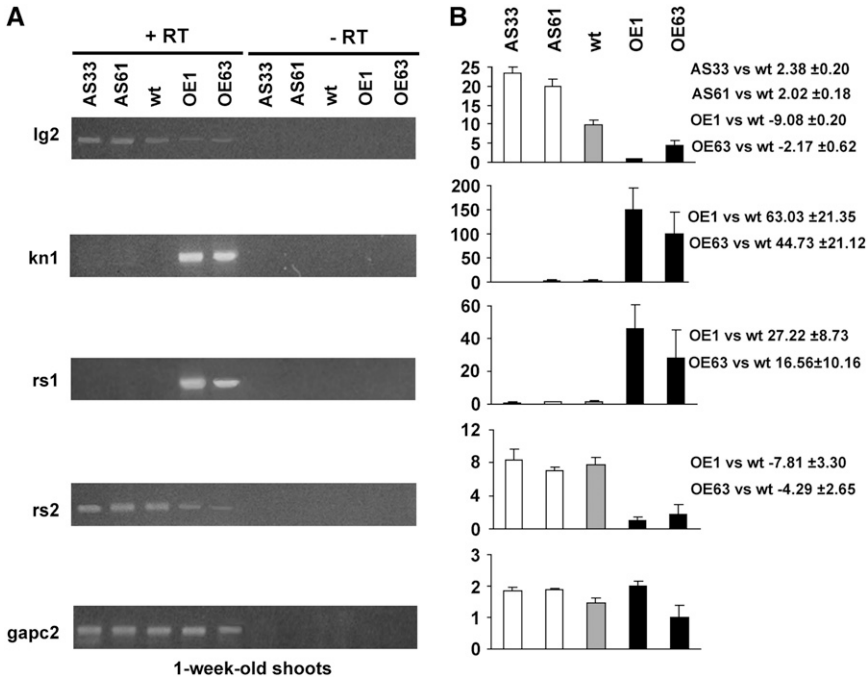

Figure 5. HDA101 Affects Transcription of Genes Involved in the Control of Plant Development.

(A) RNA extracted from 1-week-old shoots was used for semiquantitative RT-PCR analysis of transcripts with (+) or without (−) reverse transcriptase (RT). For each primer combination, the PCR was conducted under nonsaturating conditions. Representative ethidium bromide–stained gel pictures are shown and indicate that the transcript levels of *lg2*, *kn1*, *rs1*, and *rs2* genes are affected in *hda101* mutants compared with the wild type. *gapc2* is shown as an example of a gene whose transcription is similar in wild-type and mutant plants.

(B) The precise quantification of the transcript level of genes showed in **(A)** was evaluated by real-time RT-PCR analysis. Bar diagrams represent the mean values of transcript amount standardized to the transcript amount of *gapc2* (see Methods for details) and obtained by analysis performed using two different cDNA preparations and at least three replicates for each preparation. Ordinates are fold differences compared with the sample with lower transcript level; SE is reported. For sequences showing statistically significant (F test; $P < 0.05$) differential expression, the AS versus the wild type and OE versus the wild type ratios are indicated.

sequences was unaffected. Interestingly, the 5′-end and coding regions of the *lg2* and *rs2* genes, but not sequences of *kn1* and *rs1* genes, showed differences in their histone acetylation level. Both *lg2* and *rs2* exhibited a high histone acetylation status in wild-type plants (see Supplemental Figure 6 online). Up- and downregulation of *hda101* determined hypo- and hyperacetylation of *lg2*, respectively, while only reduction of H3ac and/or H4ac level in the OE1 line was observed for *rs2* (Table 4; see Supplemental Figure 6 online).

The seven genes showing changes in histone acetylation levels belong to only three of the nine classes, which describe gene expression profiles in *hda101* mutants with respect to the wild type (Tables 2 and 4). In particular, the comparison between histone acetylation and expression profiles revealed that the four genes exhibiting hyperacetylation in the AS33 line displayed a concomitant increase of their transcript levels relative to the wild type (the three class A and the single class B members in Table 4). On the contrary, six of the seven hypoacetylated genes in the OE1 line exhibited a parallel reduction of their transcript level (the three class A and three class I members in Table 4). Nevertheless, one gene, the TC257813 (class B) sequence, was hypoacetylated in the OE1 line without showing concomitant changes in its mRNA amount. Overall, these findings indicate that only a subset of genes displaying different expression in *hda101* transgenic mutants also exhibit differences in histone acetylation levels. Usually, but not always, HDA101 activity is inversely correlated with transcription of these genes.

HDA101 Effect on Histone Modifications Other Than Acetylation

The HDA101 effect on histone modifications other than acetylation was analyzed in the 12 repetitive and 27 nonrepetitive sequences by means of ChIP assays with antibodies specific for H3K4me2, H3K9me2, and H3S10ph. Results showed that chromatin regions of repeats and of some genes are characterized by the concomitant presence of significant levels of H3ac/H4ac and H3K9me2 (see Supplemental Figures 5 and 6 online). Levels of H3K4me2 significantly higher than background were observed in most of the genes considered and in some of the repeats that exhibited transcription activity (Table 3; see Supplemental Figures 5 and 6 online). Variations in the levels of at least one among H3K4me2, H3K9me2, and H3S10ph were observed in *hda101* transgenic mutants for seven out of 12 repeats and all seven genes that exhibited change in their histone acetylation levels (Tables 3 and 4). No differences in the levels of the three histone

Table 3. Real-Time PCR Quantification of ChIP Assays for Repeats

		AS33 versus Wild Type					OE1 versus Wild Type				
Repetitive Sequence	Exp. Level[a]	H3ac	H4ac	H3K4me2	H3K9me2	H3S10ph	H3ac	H4ac	H3K4me2	H3K9me2	H3S10ph
Cinful	+	2.49 ± 0.37	2.17 ± 0.26	/	/	/	/	/	/	/	/
Huck2	−	1.81 ± 0.07	/	/	/	/	/	/	/	/	/
Opie2	+	/	/	/	/	/	/	/	/	/	/
Mu TIR	+	1.62 ± 0.06	3.91 ± 0.15	/	−1.23 ± 0.05	/	−2.44 ± 0.19	−1.57 ± 0.12	/	/	/
MuDRa	+	/	/	/	/	/	/	/	/	/	/
CentC	ND	2.14 ± 0.02	2.73 ± 0.13	/	/	1.31 ± 0.12	−2.30 ± 0.03	/	/	/	−1.31 ± 0.04
CRM2 GAG	+	3.44 ± 0.10	4.86 ± 0.10	2.07 ± 0.05	−1.63 ± 0.03	2.37 ± 0.12	/	/	/	/	/
CRM2 LTR	−	3.73 ± 0.05	2.41 ± 0.14	/	/	/	/	/	/	/	/
rDNA 5S	+	/	1.87 ± 0.16	/	−1.62 ± 0.09	1.29 ± 0.02	−1.74 ± 0.03	−1.47 ± 0.06	/	/	/
rDNA 26S	+	2.02 ± 0.12	3.63 ± 1.29	2.96 ± 0.14	/	2.43 ± 0.15	−2.50 ± 0.17	−2.08 ± 0.29	−1.69 ± 0.08	1.88 ± 0.26	−2.30 ± 0.56
rDNA 26/18S	+	1.87 ± 0.20	3.00 ± 0.21	1.80 ± 0.20	/	/	−1.52 ± 0.02	−1.70 ± 0.30	/	2.76 ± 0.20	/
TC254543[b]	−	1.72 ± 0.07	2.43 ± 0.07	1.72 ± 0.15	/	1.56 ± 0.02	/	/	/	/	/

[a] Expression level is semiquantitative evaluation of repeat expression in the wild type; + indicates amplification and – indicates no amplification of the corresponding cDNA fragments after 40 cycles in RT-PCR analysis, as visualized in ethidium bromide–stained agarose gel. ND, not determined.
[b] TC254543 is the only repeat with different expression in AS lines, while mRNA level in OE lines is similar to the wild type.
H3 cter corrected data are shown (see text and Methods for details). At least two independent ChIP assays and three real-time PCR repetitions for each assay were performed. Data indicate the mean values and SE of fold differences between immunoprecipitates of transgenic lines and the wild type. Only statistically significant differences (F test; $P < 0.05$) are reported; a slash represents no significant variation.

marks were observed for sequences with unchanged H3ac and/or H4ac levels (data not shown). These results indicate that the alteration of *hda101* expression not only affects histone acetylation but also induces changes in the three histone modifications other than acetylation analyzed herein. Specifically, the data showed that hyperacetylation correlated with the increase of H3K4me2 and/or H3S10ph and/or with the decrease of H3K9me2, while the opposite correlation was observed for hypoacetylation. No exception to this rule was observed. Nevertheless, these results also show that different sequences exhibit distinct combinations of changes in the levels of H3K4me2, H3K9me2, and H3S10ph. For example, OE1-related hypoacetylation of *26S rDNA* genes affected all three histone modifications, while only an increase of H3K9me2 was observed in hypoacetylated *26/18S* rDNA intergenic spacer regions. This observation indicates that alteration of *hda101* expression affects H3K4me2, H3K9me2, and H3S10ph in a sequence-specific manner.

In addition, a possible effect of HDA101 on DNA methylation was analyzed using both McrBC-based and DNA gel blot analysis. McrBC is an enzyme that digests DNA methylated at two or more cytosines, thus reducing PCR amplification proportionally to the level of DNA methylation in the sequence encompassed by the selected primers (Lippman et al., 2005). This analysis showed that neither repeats nor genes exhibited relevant changes in their DNA methylation pattern in *hda101* transgenic mutants versus the wild type (see Supplemental Table 1 online). Similar results were obtained in DNA gel blot analysis following digestion of genomic DNA with the methylation-sensitive *Hpa*II and *Msp*I enzymes (data not shown).

DISCUSSION

In this study, we describe the characterization of transgenic maize mutants with up- and downregulation of *hda101* expression due to constitutive overexpression of sense and antisense transcripts, respectively. The perturbation of *hda101* expression induced morphological and molecular phenotypic alterations. These effects were transient because a wild-type phenotype was restored when normal *hda101* expression was reestablished in segregants devoid of the transgene. Our results provide evidence that HDA101 reversibly regulates histone acetylation, thus participating in the control of gene and repeat activity, the setting of the histone code, and the modulation of developmental programs.

Differences and Distinct Information from Transgenic Mutants with Upregulation and Downregulation of *hda101* Expression

Constitutive overexpression of *hda101* sense or antisense transcripts provokes different effects, which do not merely result in opposite phenotypes. Plants from AS and OE lines exhibited both similar and different phenotypes. Furthermore, transcript and histone acetylation levels of some of the analyzed sequences were affected only in one type of mutant but not in the other. This observation can be simply explained because, for example, reduction of mRNA cannot be observed for a sequence that was not transcribed in wild-type seedlings. However, this does not account for all data reported. Expression of the endogenous *hda101* gene occurs in all tissues, although mRNA levels differ with development (Varotto et al., 2003). Hence, constitutive antisense-mediated downregulation specifically affects transcription in cells expressing *hda101*, whereas upregulation occurs in all cell types. Furthermore, stoichiometry of HDA101-containing complexes can be differently affected by removing or by increasing HDA101 protein. In this context, AS and OE lines provide distinct information, and both have been proven to be useful tools to analyze HDA101 function.

HDA101-Mediated Control of Gene and Repeat Expression

Results from RT-PCR analysis indicated that HDA101 both positively and negatively affected transcription of 19 of the

Table 4. Real-Time PCR Quantification of ChIP Assays for Nonrepetitive Sequences

Exp. Group[a]	Nonrepetitive Sequence	AS33 versus Wild Type					OE1 versus Wild Type				
		H3ac	H4ac	H3K4me2	H3K9me2	H3S10ph	H3ac	H4ac	H3K4me2	H3K9me2	H3S10ph
A AS33 and AS61 > wt OE1 and OE63 < wt	*lg2*	2.69 ± 0.64	/	/	/	/	−1.70 ± 0.40	−1.89 ± 0.38	/	/	/
	lg2 promoter	1.80 ± 0.19	2.07 ± 0.11	2.35 ± 0.02	/	/	−2.70 ± 0.33	/	−2.08 ± 0.30	/	/
	TC313780	1.66 ± 0.07	/	1.66 ± 0.11	/	/	−1.67 ± 0.08	−1.85 ± 0.04	/	1.82 ± 0.14	/
	AZM5_22022 promoter[b]	1.87 ± 0.08	2.16 ± 0.20	/	/	/	−2.32 ± 0.11	−1.88 ± 0.06	−1.83 ± 0.13	1.75 ± 0.05	/
	T18745	3.44 ± 0.47	3.1 ± 0.22	1.62 ± 0.11	−1.75 ± 0.03	1.82 ± 0.24	−2.64 ± 0.84	/	/	1.70 ± 0.09	/
B AS33 and AS61 > wt OE1 and OE63 = wt	TC257813	2.27 ± 0.03	1.70 ± 0.09	4.24 ± 0.02	−5.56 ± 1.11	4.19 ± 0.42	−2.50 ± 0.27	/	−5.56 ± 0.97	/	/
I AS33 and AS61 = wt OE1 and OE63 < wt	TC251766	/	/	/	/	/	−2.43 ± 0.02	−2.77 ± 0.08	−2.22 ± 0.14	/	/
	TC248146	/	/	/	/	/	−8.30 ± 1.70	−3.57 ± 0.43	−3.48 ± 0.69	/	
	rs2	/	/	/	/	/	−2.86 ± 0.15	−2.38 ± 0.03	−1.92 ± 0.08	/	/
	rs2 5′ intron	/	/	/	/	/	−2.69 ± 0.17	/	−2.56 ± 0.47	/	/
H AS33 and AS61 = wt OE1 and OE63 = wt	*gapc2*	/	/	/	/	/	/	/	/	/	/

[a] Expression class indicates sequences grouped according to statistically significant changes of their expression profiles in AS/OE transgenic mutants compared with the wild type (see Table 2).

[b] AZM5_22022 is the putative TC313780 promoter.

H3 cter corrected data are shown (see text and Methods for details). At least two independent ChIP assays and three real-time PCR repetitions for each assay were performed. Data indicate the mean values and SE of fold differences between immunoprecipitates of transgenic lines and the wild type. Only statistically significant differences (F test, $P < 0.05$) are reported; a slash represents no significant variation. Chromatin extracted from 1-week-old shoots was employed for *lg2* and *rs2* genes; for all other sequences, chromatin was used from 2-week-old seedlings.

nonrepetitive sequences analyzed in this study. Histone deacetylation is typically considered to play a role in transcriptional repression/gene silencing. For any given gene, if HDA101 had a direct (repressive) effect on expression, one would expect to see less expression and higher histone acetylation in OE lines and more expression with lower histone acetylation in AS lines. Seven of the nonrepetitive genes analyzed showed this pattern. For the other 12 nonrepetitive genes, transcript levels, but not histone acetylation levels, were altered in *hda101* mutants. This pattern suggests an indirect effect, possibly due to HDA101-mediated repression of an upstream regulator (Thiagalingam et al., 2003) or some type of transcription-coupled recruitment of HDA101 activity similar to the H3 Lys methylation reported to accompany transcriptional elongation in budding yeast and mammals (Eissenberg and Shilatifard, 2006).

For one gene (the TC257813 sequence in the OE1 line) and for most of the repetitive sequences analyzed, the *hda101* mutants showed altered histone acetylation but no effect on transcript levels. This pattern was observed for repeats that differed not only in expression level (ranging from highly expressed rDNA genes to poorly expressed transposable elements) but also in the RNA polymerases responsible for their transcription (transposable elements transcribed by RNA polymerase II, 26S rDNA repeats by RNA polymerase I, and *5S rDNA* genes by RNA polymerase III). This result suggests that the observed changes in histone acetylation are not due to some general effect exerted by transcription but instead are a direct consequence of altered HDA101 activity. These observations agree with previous findings from *Arabidopsis*, showing that changes in histone acetylation do not necessarily coincide with altered gene expression (Probst et al., 2004; Tian et al., 2005). Recent studies suggest that this may be due to the need for cumulative acetylation of multiple Lys residues to form open transcriptionally active chromatin (Henikoff, 2005; Schubeler and Turner, 2005). Hence, the perturbation of *hda101* expression alone might not be sufficient to affect the chromatin structure of highly packaged heterochromatin-like repeats. The activity of other members of the HDAC family might be necessary to deacetylate specific Lys residues and to obtain the cumulative effect required for repression. Alternatively, specific levels or combinations of modifications other than acetylation may override the acetylation status of most of the repeats and of some genes, making transcription of these sequences insensitive to changes in the H3ac/H4ac levels induced by the perturbation of *hda101* expression. For example, in repeats, histone deacetylation alone may not account for the regulation of expression in heterochromatic regions, as an efficient transcript repression may only be achieved through the participation of additional histone modifying enzymes or distinct regulatory mechanisms.

HDA101 Participation in Setting the Histone Code

Our results indicate that HDA101 affected levels of H3K4me2, H3K9me2, and H3S10ph. This was observed in genes, showing concomitant changes of expression, and in repeats, without alteration of transcript levels. As predicted by the histone code

hypothesis (Strahl and Allis, 2000; Margueron et al., 2005), hyperacetylation in AS33 plants correlated with enrichment of H3K4me2 and H3S10ph and with reduction of H3K9me2, while the opposite correlation was observed upon hypoacetylation in OE1 plants. However, ChIP assays indicated that only a subset of hyper- or hypoacetylated sequences showed concomitant changes in the levels of the three histone modifications analyzed. In particular, different sequences exhibited distinct combinations of changes of the levels of H3K4me2, H3K9me2, and H3S10ph. Therefore, it can be deduced that HDA101 participates in setting the histone code by affecting histone modifications other than acetylation in a sequence-specific manner. According to previous indications from biochemical characterization (Kolle et al., 1999), we found that HDA101 exhibited substrate preferences for Lys residues, and in some of the sequences analyzed, it affected either H3ac or H4ac. A sequence-specific pattern of histone modifications might influence HDA101 substrate specificity (Fischle et al., 2003; Peterson and Laniel, 2004). On the other hand, sequence-specific distinct combinations of acetylated Lys residues might act as a unique signal for the recruitment of enzymes modifying histone methylation and phosphorylation.

Additional information about the effect HDA101 exerts on histone modifications arises from the finding that it altered nuclear distribution of H3K9me2. According to previous indications from large-genome plant species (Houben et al., 2003), we observed that in wild-type interphase nuclei, H3K9me2 is uniformly distributed along the whole chromatin. Conversely, Shi and Dawe (2006) presented results indicating that in maize nuclei, H3K9me2 was associated with euchromatin. In many species, H3K9me2 is considered a heterochromatin mark, and Houben et al. (2003) suggested that its widespread distribution in large-genome species is related to a high amount of retroelements. In agreement with this scenario, our data from ChIP assays revealed that high levels of H3K9me2 were observed in most of the repeats, although it was also present in some of the nonrepetitive sequences analyzed. It is worth noting that immunostaining experiments from our laboratory and from Houben et al. (2003) were performed using interphase nuclei prepared from maize root apexes, while preparations of Shi and Dawe (2006) were from tapetal cells. Therefore, a possible reason of the different observations reported by these laboratories might be related to differences of the H3K9me2 nuclear localization profile in distinct cell types. Apart from these indications on the nuclear localization of H3K9me2 in wild-type nuclei, our results show that nuclear distribution but not total level of H3K9me2 was affected in *hda101* mutants. This finding suggests that HDA101 might provoke the nuclear redistribution of H3K9me2 by affecting histone exchange. The relative tendency of AS and OE mutants to nucleosome loss and enrichment, respectively, support an involvement of HDA101 in histone deposition and redistribution. Indeed, HDAC activities have been found in complexes required for both DNA synthesis–dependent and -independent nucleosome assembly (Loyola and Almouzni, 2004).

HDA101 Function in Plant Development

Results from phenotypic and molecular analysis provide some indications about HDA101's role in plant development. *Hda101* transgenic mutants exhibited several morphological and developmental defects, spanning from plant and flower architecture to kernel size and production. In particular, *hda101* transgenic mutants displayed a slow growth rate compared with wild-type plants, resulting in adult plants that were delayed in flowering and reduced in height. This phenotype might be related to defects in controlling vegetative-to-reproductive phase transition. Indeed, the transcript and histone acetylation levels of the *lg2* gene, which is involved in the control of this transition (Walsh and Freeling, 1999), were inversely related to *hda101* expression in *hda101* transgenic mutants. In addition, a characteristic dwarf phenotype with development of normally suppressed axillary branches was observed in plants overexpressing *hda101* and was particularly pronounced in the OE1 line. In 1-week-old shoots of OE lines, but not in wild-type and AS lines, the transcripts of *kn1* and *rs1* homeobox genes were detected, although the histone acetylation status in their promoter and coding regions was unaffected. Upregulation of *hda101*, however, induced hypoacetylation and reduced expression of *rs2*, a negative regulator of *kn1* and *rs1* transcription (Timmermans et al., 1999; Tsiantis et al., 1999). A recent report indicates that the RS2 protein and its *Arabidopsis* ortholog ASYMMETRIC LEAVES1 interact with components of an epigenetic-related regulatory machinery, including the chromatin remodeling protein HIRA, and suggests that this complex silences *knotted*-like genes, thus establishing determinacy during leaf development (Phelps-Durr et al., 2005). In this study, we show that HDA101 is also involved in this regulatory mechanism. The reduction of *rs2* transcription and concomitant ectopic expression of *kn1* and *rs1* are expected to induce uncontrolled proliferation of cells and formation of ectopic meristems (Smith et al., 1992; Chuck et al., 1996). This might be related to proliferation of normally suppressed axillary branches in most of the OE mutant plants.

Our results suggest that HDA101 is involved in controlling meristem formation and transition from vegetative to reproductive phase. It remains to be established which of the developmentally expressed genes, showing alteration of their transcripts and histone acetylation levels in *hda101* mutants, are the direct targets of HDA101 activity. The detailed biochemical characterization of HDA101-containing complexes is required to shed light on the precise mechanisms of HDA101 action. Furthermore, it is worth noting that many of the specific phenotypes evident in *lg2*, *kn1*, *rs1*, and *rs2* knockout mutants were not observed in the *hda101* transgenic lines. For example, *hda101* mutant plants did not show variation in leaf number, which is a characteristic of almost all maize mutants affecting phase transition (Poethig, 2003). In *hda101* mutants, the reduction in plant height was due to shorter internodes, and the delay in flowering time is probably related to a general effect on growth rate and leaf/inflorescence initiation. Evidence from this study and from previous reports (Rossi et al., 2003; Varotto et al., 2003) indicates that HDA101 can, either directly or indirectly, affect the expression of genes involved in various pathways. However, how these pathways intersect and how their perturbation, through alteration of HDA101 activity, contributes to determine the phenotypes observed in *hda101* mutants is not yet understood and needs to be further investigated.

Functional Similarities and Differences between *hda101* and *Arabidopsis Rpd3*-Type Genes

Results from this study support previous evidence obtained through phylogenetic analysis, indicating that *hda101* is the maize ortholog of the *Arabidopsis HDA19* gene (Pandey et al., 2002; Varotto et al., 2003). These genes share features that distinguish them from another member of the *Arabidopsis* Rpd3-family, the *HDA6* gene. Specifically, both *hda101* and *HDA19* exhibit pleiotropic effects on development and gene transcription, affect total levels of acetylated histones, and do not impair transcript levels and DNA methylation of most of the repeats (Tian and Chen, 2001; Tian et al., 2003, 2005). Conversely, *HDA6* knockout mutants do not exhibit a drastic phenotype and reduction of H4ac levels, while displaying an altered transcription and DNA methylation of specific repeats (Lippman et al., 2003; Probst et al., 2004). Nevertheless, our results point out some differences between HDA101 and HDA19 enzymes. First, HDA101 affects levels of H4K5ac, while HDA19 does not. Second, *hda101* mutants affect histone acetylation levels also within coding regions, whereas HDA19 influences histone acetylation predominantly at promoters. Third, wild-type level of H3K4me2 is reestablished in plants upon loss of HDA101 transgenes, while alterations in methylated histones were stably inherited in plants with restored *HDA19* expression. It is unclear whether HDA19, like HDA101, affects histone acetylation within repeats because these data are lacking. In addition, HDA19 is localized exclusively in the nucleus (Zhou et al., 2005; Fong et al., 2006), whereas HDA101 exhibits a nucleus-cytoplasmic localization profile influenced by cell type and developmental stages (Varotto et al., 2003; S. Varotto and V. Rossi, unpublished data). These differences suggest that the two Rpd3 orthologs may partially diverge in activity and substrate specificities. In this study, we show that maize and *Arabidopsis* differ with respect to the distribution of modified histones in interphase nuclei, since in maize, H4ac and H3K9me2 are not confined to poorly and highly DAPI-stained regions, respectively, but spread across the whole chromatin. Accordingly, ChIP assays showed that these histone marks coexist within the same chromatin region of many genes and repeats. In this context, at least a partial degree of functional diversification between *hda101* and *HDA19* might be an important requirement, related to different chromatin organizations in maize and *Arabidopsis*.

METHODS

Plasmids, Maize Transformation, and Crossing Scheme

The constitutive maize (*Zea mays*) ubiquitin promoter (Christensen et al., 1992) was cloned upstream or downstream of the full-length *hda101* cDNA sequence, into the pGEM3-Zm Rpd3I plasmid (Rossi et al., 2003), to obtain sense and antisense *hda101* constructs, respectively. The polyadenylation domain of the *nos* gene was inserted opposite to the *ubiquitin* promoter. In the antisense plasmid, the 250-bp 3′-end region of the *hda101* cDNA, corresponding to probe R101, was deleted by *Spe*I restriction. Therefore, this probe, which is specific for the *hda101* member of the Rpd3 family (Varotto et al., 2003), was used in RNA gel blot analysis allowed specific detection of the endogenous *hda101* transcript in AS transformants. The resulting cassettes were used to generate the pRpd3-53 and pRpd3-35 plasmids (Figure 1A). These plasmids were employed to transform protoplasts from maize suspension cell line HE-89 (Morocz et al., 1990) using the polyethylene glycol method. Two weeks after protoplast transformation, the microcalli were plated on agar-solidified medium containing 200 mg/L DL-gluphosinate. Transgenic cell clones were subcultured in the presence of gluphosinate. Transgenic callus lines were further screened for the presence of the transgene by PCR using the following primer combinations: PUbi1 (5′-TCGACGAGTCTAACGGACACC-3′) plus Rpd3-53 (5′-CCTCGCACTTCTTGGCGTGG-3′) and PUbi1 plus Rpd3-35 (5′-GAAGAGTCATCGAGGAGGAGC-3′).

Regenerated T0 plants were first converted to the B73 recurrent parent by two sequential backcrosses to minimize mixed genetic background influence (BC-T1 and BC-T2 generations). After backcrosses, plants were selfed twice to obtain the T3 and T4 generations that are heterozygous and homozygous, respectively, for the presence of the transgene. The T4 homozygous plants were then selfed twice to produce the T5 and T6 generations of homozygous plants, which were used for phenotypic and molecular analysis. In parallel, the T4 homozygous plants were also backcrossed twice to the B73 inbred. The two backcrosses originated the following plant generations: first, the BC-T5 generation (indicated as BC-T5 he) heterozygous for the presence of the transgene; second, the BC-T6 generation that segregated in heterozygous plants (BC-T6 he) and wild-type plants (BC-T6 wt) that have lost the transgene due to genetic segregation. The presence of the transgene in segregating plants was assessed for resistance to gluphosinate and using PCR screening.

Phenotypic Analysis

Phenotypic analysis was performed on plants grown in the greenhouse and during field trials under containment, according to guidelines of the Italian laws for biosafety. The analysis was performed using plants from different generations: T5 and T6 homozygous, BC-T5 he and BC-T6 he heterozygous, and wild-type and BC-T6 wt devoid of the transgene. A minimum of 20 plants for each independent transformant was monitored daily for germination, plant traits, and flowering onset. The days to flowering were calculated as GDD $=$ [(Tmax $+$ Tmin)/2] – 10 from coleoptile emergence to onset of pollen shed and silk appearance. The average value of daily GDD accumulations, under growing conditions adopted in this study, was 13. Analysis of adult plant, inflorescence, and kernel traits was performed according to indication of the International Board for Plant Genetic Resource. Seedling dry weight, first internode length, root dry weight, and root apical length were measured on greenhouse-grown 2-week-old seedlings, which correspond at the two-leaf stage for most of the wild-type seedlings. Statistical analysis was performed by applying Student's *t* tests.

DNA, RNA, Protein, and Histone Blot Analysis

Procedures for genomic DNA, RNA, and protein extraction as well as DNA, RNA, and protein blot analysis were previously described (Rossi et al., 1998; Varotto et al., 2003). All materials were prepared from 2-week-old maize seedlings and shoots harvested 5 to 7 d after sowing. These shoots, named 1-week-old shoots and ~1.5 to 2 cm in length, were obtained by cutting immediately above the coleoptile node; thus, all the above-ground tissues and meristems were sampled. Genomic DNA was restricted and blots hybridized as indicated in Supplemental Figure 1 online. Probes specific for different Zm *Rpd3* members and employed both in DNA and RNA gel blot analysis were described by Varotto et al. (2003). The *hda101*-specific DNA sense probe used for detecting antisense transcript was generated by linear PCR in the presence of α-^{32}P-dCTP and using an *hda101*-specific sense primer, located in the ATG region. Production and characterization of the anti-ZmRpd3 antibody was previously described (Varotto et al., 2003). Histone was extracted from

2-week-old seedlings and blotted as described by Tariq et al. (2003). The amount of histone extracts was quantified using Bradford assay and further evaluated by visual checking of the Coomassie Brilliant Blue–stained SDS-PAGE. The antibodies specific for the histone modifications analyzed in immunoblots, immunostainings, and ChIPs were purchased from Upstate: α-H3ac (06-599), α-H4ac (06-866), α-H3K9ac (07-352), α-H3K14ac (07-353), α-H4K5ac (06-759), α-H4K8ac (06-760), α-H4K12ac (06-761), α-H4K16ac (06-762), α-H3K4me2 (07-030), α-H3K9me2 (07-212), and α-H3S10ph (06-570). α-H3 cter (ab1791) was purchased from Abcam.

Immunostaining and Electron Microscopy Scanning

For immunostaining root apexes of 3- to 5-d-old AS33, OE1 and wild-type seedlings were fixed in 4% paraformaldehyde and 0.1 M PBS for 1 h. After extensive washing with 0.1 M PBS, root apexes were digested for 30 to 40 min as described (Houben et al., 2003) and squashed in polylysinated slides. Following freezing in liquid nitrogen, nuclei were blocked in 8% BSA and 0.1% Triton X-100, washed with PBS, and incubated with the appropriate antibody in a humidified chamber overnight at 4°C. Slides were washed in PBS and incubated with goat-anti-rabbit-FITC (1:50; Sigma-Aldrich) or goat-anti-rabbit-rhodamine (1:100; Upstate). Nuclei were counterstained with DAPI in Vectashield (Vector). The immunolocalization experiments with the mutants and wild type were repeated three times for each antibody. Preparations were analyzed with a Leica DM R HC fluorescence microscope equipped with a Leica DC 300F camera. The images were processed and merged with Adobe Photoshop software (Adobe Systems).

For electron microscopy scanning, maize inflorescences were fixed in 3% gluteraldheyde in 0.1 M cocodilate buffer, pH 6.9, for 16 h at 4°C and postfixed in 1% OsO_4 in the same buffer for 1 h at 4°C. The samples were dehydrated in an ethanol series to 100% ethanol, critical point dried, sputter coated with gold, and viewed on a Cambridge scanning electron microscope at an accelerating voltage of 150 kV.

cDNA Synthesis and Semiquantitative RT-PCR Analysis

Equal amount of total RNA was used for cDNA synthesis as described (Varotto et al., 2003), and one-tenth dilution was used for RT-PCR. Semiquantitative RT-PCR analysis was conducted under nonsaturating amplification conditions; the number of amplification cycles corresponding to these conditions was estimated for each of the primer combinations used. Amplified fragments were loaded into 1.5% agarose gel, electrophoretically fractionated, and visualized through ethidium bromide staining.

ChIP Assays

ChIP was performed as described (Tariq et al., 2003) with minor modifications. Leaves of 2-week-old maize seedlings or 1.5- to 2-cm 1-week-old shoots were fixed with 1% formaldehyde in TS buffer (200 mM NaCl and 20 mM Tris-HCl, pH 7.6) immediately after harvesting. Fixation was conducted at 4°C, using three cycles consisting each of 2 min of vacuum infiltration plus 8 min of rest in TS buffer, for a total of 30 min. Fixation was blocked with 0.1 M glycine, and leaves or shoots were washed, ground to powder in liquid N_2, suspended in lysis buffer (50 mM HEPES, pH 7.5, 150 mM NaCl, 1 mM EDTA, 1% Triton X-100, 0.1% deoxycholate, 0.1% SDS, 1 mM PMSF, 10 mM Na butyrate, 1 μg/mL aprotinin, and 1 μg/mL pepstatin A), filtered, and washed twice in lysis buffer. Approximately 0.5 g of 2-week-old leaves and 0.35 g of 1-week-old shoots are required to extract 25 μg of chromatin, corresponding to the amount required for one ChIP assay. The extracted DNA was sheared by sonication to ~500- to 1000-bp fragments and centrifuged, and supernatants were carefully quantified using a spectrophotometer. A fraction of the supernatants was saved and after cross-linking reversion (see below) used as input in PCR evaluation. For any ChIP assay, 25 μg of chromatin from mutants and the wild type were precleared with 60 μL salmon sperm DNA/Protein A agarose (Upstate) for 3 h at 4°C and centrifuged, and the histone-DNA complexes were immunoprecipitated overnight at 4°C adding the appropriate antibody. Typically, 5 μL of α-H3 cter (Abcam; ab1791) and α-H3ac (Upstate; 06-599) and 10 μL of α-H4ac (Upstate; 06-866), α-H3K4me2 (Upstate; 07-030), α-H3K9me2 (Upstate; 07-212), and α-H3S10ph (Upstate; 06-570) were used for immunoprecipitation. Sixty microliters of salmon sperm DNA/Protein A agarose was then added and incubation continued for 2 h. The agarose beads were subsequently washed once with low salt buffer (20 mM Tris-HCl, pH 8, 150 mM NaCl, 1% Triton X-100, 2 mM EDTA, and 0.1% SDS), three times with high salt buffer (20 mM Tris-HCl, pH 8, 500 mM NaCl, 1% Triton X-100, 2 mM EDTA, and 0.1% SDS), once with LNDET buffer (10 mM Tris-HCl, pH 8, 250 mM LiCl, 1% Nonidet P-40, and 1% sodium deoxycholate), and twice with Tris-EDTA buffer; the chromatin was eluted with 0.1 M $NaHCO_3$ and 1% SDS. Cross-linking was reversed 4 h at 65°C in the presence of 0.2 M NaCl; samples were treated with proteinase K for 1 h, extracted twice with phenol-chloroform and once with chloroform, and DNA was resuspended in 75 μL of Tris-EDTA. One microliter of ChIP DNAs and one-tenth dilution of inputs were used for PCR analysis. At least two independent ChIP experiments were performed for each antibody, and at least three repetitions of PCR analysis were performed for each experiment and for each sequence analyzed. ANOVA was applied to data obtained by real-time PCR analysis (see below) to identify statistically significant changes ($P < 0.05$) in the amount of the immunoprecipitated sequences between *hda101* mutants and the wild type.

Analysis of DNA Methylation

For McrBC analysis of DNA methylation, 1 μg of sonicated genomic DNA (with average size of 500 to 1000 bp) was incubated with 50 units of McrBC enzyme (New England Biolabs), according to manufacturer's instructions, at 37°C overnight; 10 ng of McrBC-treated and untreated DNA was used for PCR. For DNA gel blot analysis, genomic DNA was restricted with the methylation-sensitive isoschizomers *Hpa*II ($^{m}C^{m}CGG$) and *Msp*I ($^{m}CCGG$), fractionated on 1% agarose gel, blotted, and hybridized with *hda101*-specific probes (Varotto et al., 2003).

Microarray Analysis

Microarray experiments were performed using slides from the Maize Oligonucleotide Array Project (http//www.maizearray.org). For wild-type, AS33, and OE1 lines (considered as the three sample treatments) a pool of 20 2-week-old seedlings were randomly divided into four independent subsets of five plants, corresponding to the four different biological replicates and used to prepare total RNA. Upon labeling of total RNA, probes derived from subsets were used to hybridize microarray slides following an interconnecting loop design (four hybridizations for each sample treatment: two with Cy3 and two with Cy5 labeling). Target labeling via RNA amplification and hybridization were in accordance to standard protocols posted on the Maize Microarray Project website (http//www.maizearray.org). Slides were analyzed and imaged and raw data obtained with the aid of a Genepix 4100A scanner (Axon). Data were normalized and statistically analyzed using tools from the Bioconductor Project (http://www.bioconductor.org; Gentleman et al., 2004), applying the following linear mixed ANOVA model using the Limma package (Smyth, 2004):

$$y_{ijkg} = \mu + A_i + D_j + (AD)_{ij} + G_g + (AG)_{ig} + (DG)_{jg} + V_k + (DV)_{jk} + (VG)_{kg} + e_{ijkgh},$$

where y_{ijkg} is the log intensity value for the g^{th} gene from pool h on array i with dye j and treatment k; μ is the overall mean across all factors; A_i is the

overall effect of array i; D_j is the overall effect of dye j; G_g is the overall effect of gene g; V_k is the overall effect of mutants k; $(AD)_{ij}$ is the array and dye interaction term; $(AG)_{ig}$ is the array-by-gene effect; $(DG)_{jg}$ is the dye-by-gene effect; $(DV)_{kg}$ is the dye-by-mutant effect; $(VG)_{kg}$ is k^{th} treatment effect of the g^{th} gene to test whether gene expression differences between treatments are various between genes. e_{ijkgh} is a random residual error term assumed normally distributed with mean 0 and variance σ_g^2 (i.e., each gene is assumed to have its own residual variance, which is shrunk toward a common distribution using an empirical Bayes model [Smyth, 2004]). To correct for accumulation of Type I error through multiple testing, a false discovery rate (Benjamini and Yekutieli, 2001), at a P value cutoff < 0.05, was employed, and all P values used are in actuality adjusted q-values.

Real-Time PCR

Samples from cDNA synthesis, ChIP, and McrBC treatment were used as templates in PCR analysis, using various primer combinations (see Supplemental Table 2 online). Each combination was tested for efficiency and specificity in PCR using genomic DNA from the wild type as a template, followed by sequencing of the amplified fragments. The accurate quantification of cDNA-, ChIP- and McrBC-related templates was performed using an iCyclerIQ (Bio-Rad) for real-time PCR analysis. PCR conditions for different samples and primer combinations are available upon request. The amplification was assessed by monitoring SYBR Green I (Sigma-Aldrich) incorporation, according to iCyclerIQ manufacturer's recommendations. Real-time PCR data analysis was performed as follows. The relative proportions of templates in each sample were determined based on the threshold cycle (TC) value for each PCR reaction. The TC value is determined as the cycle at which fluorescence rises 10 times above the mean standard deviation of background levels in all reaction wells. At least three replicates were performed for each sample during the same PCR, and a TC mean value and a standard error were obtained. A ΔTC value was calculated by subtracting the TC mean value for the samples to be compared (AS or OE mutants versus the wild type). Fold differences (FDs) for a given primer combination were then determined by raising 2 to the ΔTC power (fold differences mutant versus the wild type $= FD_{mutant} = 2[TC_{wt} - TC_{mutant}]$). In many cases two to three serial PCR experiments (see below) were performed and the mean value was considered. Subsequently, according to the template's nature, different procedures were followed. Specifically, for real-time RT-PCR to account for possible differences in cDNA synthesis and amplification efficiency, the data were standardized to the transcript amount of *gapc2* or *ac1* genes in AS, OE, and wild-type lines; these genes do not show significant differences in transcript levels in both mutants and the wild type as evaluated by microarrays (data not shown) and agarose-gel-PCR semiquantitative analysis (Figure 5). The above-described equation was applied for the *gapc2* gene (similar results were obtained using *ac1*) to obtain $FD(gapc2)_{mutant}$. The standardized FD was then calculated as $FD_{mutant}/FD(gapc2)_{mutant}$. The same procedure was used for real-time ChIP, except that FD was standardized to input chromatin: $FD(ChIP)_{mutant}/FD(Input)_{mutant}$. For H3 cter correction, each standardized FD obtained by ChIP assay with a given antibody and amplification with a given primer combination, was divided by the corresponding standardized FD obtained using H3 cter in the ChIP assay; hence, the equations were $\{FD(ChIP)_{mutant}/FD(Input)_{mutant}\}/\{FD(H3\ cter)_{mutant}/FD(Input)_{mutant}\}$. In Supplemental Figures 5 and 6 online, data were illustrated in bar diagrams as fold changes with respect to background signal. To this end, the ΔTC was calculated by subtracting the TC value for the sample immunoprecipitated with the antibody (TC ChIP) from the TC value for the corresponding sample, but omitting antibody in ChIP experiment (TC background). Data were subsequently standardized to input and corrected for H3 cter ChIP. When the TC ChIP was ≥ TC background, a ΔTC = 0 was considered, thus resulting in FD = 1. Accordingly, the background line in diagrams corresponds to the value 1 in ordinates. The same equations illustrated above were also used for real-time McrBC, but FD was standardized to McrBC untreated sample.

Data obtained from real-time RT-PCR and from real-time PCR of ChIP assays were subjected to ANOVA. Specifically, for real-time RT-PCR, two cDNA preparations, from two distinct biological samples, were obtained for each AS, OE, and wild-type line analyzed. At least three replicates of real-time RT-PCR were performed for each cDNA preparation. All TC values were standardized to the TC mean value of *gapc2* and the resulting values used for ANOVA. For real-time PCR of ChIP, at least two independent ChIP assays were performed for each antibody. At least three replicates of real-time PCR were performed for each assay.

For data arising from ChIP assays with H3 cter antibody and for H3 cter uncorrected data obtained by ChIP assay with other antibodies, the TC values were standardized to the TC mean value of the corresponding inputs. For H3 cter corrected data, the TC values were further divided to the TC mean value obtained with H3 cter. The standardized values were subsequently used for ANOVA. ANOVA was performed assuming biological sample replications as random effects and treatment effects (that is, effects due to genetic strains) considered as fixed effects.

Accession Numbers

The accession numbers of the major genes analyzed in this work are listed in Supplemental Table 2 online. The accession numbers of *hda101* cDNAs are AF384032 (maize cultivar B73) and AF0358115 (maize cultivar W22).

Supplemental Data

The following materials are available in the online version of this article.

Supplemental Figure 1. DNA Gel Blot Analysis of AS and OE Plants.

Supplemental Figure 2. Nuclear Distribution of H4ac, H3K4me2, and H3S10ph.

Supplemental Figure 3. HDA101 Does Not Affect Transcription of Repeats.

Supplemental Figure 4. Nucleosome Occupancy and Histone Modification Ratios in *hda101* Mutants Compared with the Wild Type.

Supplemental Figure 5. Levels of Histone Modifications in Repetitive Sequences.

Supplemental Figure 6. Levels of Histone Modifications in Nonrepetitive Sequences That Show Differential Expression in *hda101* Mutants.

Supplemental Table 1. Real-Time Quantification of DNA Methylation Level Using McrBC Assays.

Supplemental Table 2. List of Sequences Analyzed and Primers.

ACKNOWLEDGMENTS

We thank Chiara Lanzanova and Paolo Valoti for assistance in plant growth and phenotypic analysis. We thank Gideon Grafi, Alexander Kenzior, Massimiliano Lauria, and Alexandra Lusser for critical reading of the manuscript. We also thank Peter Loidl for critical reading of the manuscript and for providing the Zm Rpd3 antibody. This work was supported by special grants from Ministero dell'Istruzione, dell'Università e della Ricerca (Progetto FIRB: RBNE01TYZF) and from Ministero delle Politiche Agricole, Alimentari e Forestali (Progetto Frumisis and Progetto Zeagen). S.V. was supported by the Cofin Program 2004.

Received March 16, 2006; revised April 2, 2007; accepted April 12, 2007; published April 27, 2007.

REFERENCES

Aufsatz, W., Mette, M.F., Van Der Winden, J., Matzke, M., and Matzke, A.J. (2002). HDA6, a putative histone deacetylase needed to enhance DNA methylation induced by double-stranded RNA. EMBO J. **21:** 6832–6841.

Benjamini, Y., and Yekutieli, D. (2001). The control of the false discovery rate in multiple testing under dependency. Ann. Statist. **29:** 1165–1188.

Carrozza, M.J., Utley, R.T., Workman, J.L., and Cote, J. (2003). The diverse functions of histone acetyltransferase complexes. Trends Genet. **19:** 321–329.

Christensen, A.H., Sharrock, R.A., and Quail, P.H. (1992). Maize polyubiquitin genes: Structure, thermal perturbation of expression and transcript splicing, and promoter activity following transfer to protoplasts by electroporation. Plant Mol. Biol. **18:** 675–689.

Chuck, G., Lincoln, C., and Hake, S. (1996). KNAT1 induces lobed leaves with ectopic meristems when overexpressed in Arabidopsis. Plant Cell **8:** 1277–1289.

Colasanti, J., Yuan, Z., and Sundaresan, V. (1998). The indeterminate gene encodes a zinc finger protein and regulates a leaf-generated signal required for the transition to flowering in maize. Cell **15:** 593–603.

Dion, M.F., Altschuler, S.J., Wu, L.F., and Rando, O.J. (2005). Genomic characterization reveals a simple histone H4 acetylation code. Proc. Natl. Acad. Sci. USA **102:** 5501–5506.

Eissenberg, J.C., and Shilatifard, A. (2006). Leaving a mark: The many footprints of the elongating RNA polymerase II. Curr. Opin. Genet. Dev. **16:** 184–190.

Evans, M.M., and Poethig, R.S. (1995). Gibberellins promote vegetative phase change and reproductive maturity in maize. Plant Physiol. **108:** 475–487.

Fischle, W., Wang, Y., and Allis, C.D. (2003). Histones and chromatin cross-talk. Curr. Opin. Cell Biol. **15:** 172–183.

Fong, P.M., Tian, L., and Chen, Z.J. (2006). *Arabidopsis thaliana* histone deacetylase 1 (AtHD1) is localized in euchromatic regions and demonstrates histone deacetylase activity in vitro. Cell Res. **16:** 479–488.

Gentleman, R.C., et al. (2004). Bioconductor: Open software development for computational biology and bioinformatics. Genome Biol. **5:** R80.

Henikoff, S. (2005). Histone modifications: Combinatorial complexity or cumulative simplicity? Proc. Natl. Acad. Sci. USA **102:** 5308–5309.

Houben, A., Demidov, D., Gernand, D., Meister, A., Leach, C.R., and Schubert, I. (2003). Methylation of histone H3 in euchromatin of plant chromosomes depends on basic nuclear DNA content. Plant J. **33:** 967–973.

Hubbard, L., McSteen, P., Doebley, J., and Hake, S. (2002). Expression patterns and mutant phenotype of teosinte branched1 correlate with growth suppression in maize and teosinte. Genetics **162:** 1927–1935.

Huebert, D.J., and Bernstein, B.E. (2005). Genomic views of chromatin. Curr. Opin. Genet. Dev. **15:** 476–481.

Jang, I.C., Pahk, Y.M., Song, S.I., Kwon, H.J., Nahm, B.H., and Kim, J.K. (2003). Structure and expression of the rice class-I type histone deacetylase genes OsHDAC1-3: OsHDAC1 overexpression in transgenic plants leads to increased growth rate and altered architecture. Plant J. **33:** 531–541.

Jasencakova, Z., Meister, A., and Schubert, I. (2001). Chromatin organization and its relation to replication and histone acetylation during the cell cycle in barley. Chromosoma **110:** 83–92.

Kerstetter, R., Vollbrecht, E., Lowe, B., Veit, B., Yamaguchi, J., and Hake, S. (1994). Sequence analysis and expression patterns divide the maize knotted1-like homeobox genes into two classes. Plant Cell **6:** 1877–1887.

Kolle, D., Brosch, G., Lechner, T., Pipal, A., Helliger, W., Taplick, J., and Loidl, P. (1999). Different types of maize histone deacetylases are distinguished by a highly complex substrate and site specificity. Biochemistry **38:** 6769–6773.

Kurdistani, S.K., and Grunstein, M. (2003). Histone acetylation and deacetylation in yeast. Nat. Rev. Mol. Cell Biol. **4:** 276–284.

Kurdistani, S.K., Tavazoie, S., and Grunstein, M. (2004). Mapping global histone acetylation patterns to gene expression. Cell **117:** 721–733.

Lechner, T., Lusser, A., Pipal, A., Brosch, G., Loidl, A., Goralik-Schramel, M., Sendra, R., Wegener, S., Walton, J.D., and Loidl, P. (2000). RPD3-type histone deacetylase in maize embryos. Biochemistry **39:** 1683–1692.

Lippman, Z., Gendrel, A.V., Colot, V., and Martienssen, R. (2005). Profiling DNA methylation patterns using genomic tiling microarrays. Nat. Methods **2:** 219–224.

Lippman, Z., May, B., Yordan, C., Singer, T., and Martienssen, R. (2003). Distinct mechanisms determine transposon inheritance and methylation via small interfering RNA and histone modification. PLoS Biol. **1:** 420–428.

Loidl, P. (2004). A plant dialect of the histone language. Trends Plant Sci. **9:** 84–90.

Long, J.A., Ohno, C., Smith, Z.R., and Meyerowitz, E.M. (2006). TOPLESS regulates apical embryonic fate in Arabidopsis. Science **312:** 1520–1523.

Loyola, A., and Almouzni, G. (2004). Histone chaperones, a supporting role in the limelight. Biochim. Biophys. Acta **1677:** 3–11.

Lusser, A., Kolle, D., and Loidl, P. (2001). Histone acetylation: Lesson from the plant kingdom. Trends Plant Sci. **6:** 59–65.

Margueron, R., Trojer, P., and Reinberg, D. (2005). The key to development: interpreting the histone code. Curr. Opin. Genet. Dev. **15:** 163–176.

Messing, J., Bharti, A.K., Karlowski, W.M., Gundlach, H., Ran Kim, H., Yu, Y., Wei, F., Fuks, G., Soderlund, C.A., Mayer, K.F.X., and Wing, R.A. (2004). Sequence composition and genome organization of maize. Proc. Natl. Acad. Sci. USA **101:** 14349–14354.

Moose, S.P., and Sisco, P.H. (1994). Glossy15 controls the epidermal juvenile-to-adult phase transition in maize. Plant Cell **6:** 1343–1355.

Morocz, S., Donn, G., Nemeth, J., and Dudits, D. (1990). An improved system to obtain fertile regenerants via maize protoplasts isolated from a highly embryogenic suspension culture. Theor. Appl. Genet. **80:** 721–726.

Pandey, R., Müller, A., Napoli, C.A., Slinger, D.A., Pikaard, C.S., Richards, E.J., Bender, J., Mount, D.W., and Jorgensen, R.A. (2002). Analysis of histone acetyltransferase and histone deacetylase families of *Arabidopsis thaliana* suggests functional diversification of chromatin modification among multicellular eukaryotes. Nucleic Acids Res. **3:** 5036–5055.

Peterson, C.L., and Laniel, M.A. (2004). Histones and histone modifications. Curr. Biol. **14:** R546–R551.

Phelps-Durr, T.L., Thomas, J., Vahab, P., and Timmermans, M.C. (2005). Maize rough sheath2 and its Arabidopsis orthologue ASYMMETRIC LEAVES1 interact with HIRA, a predicted histone chaperone, to maintain knox gene silencing and determinacy during organogenesis. Plant Cell **17:** 2886–2898.

Poethig, R.S. (2003). Phase change and the regulation of developmental timing in plants. Science **301:** 334–336.

Pokholok, D.K., et al. (2005). Genome-wide map of nucleosome acetylation and methylation in yeast. Cell **122:** 517–527.

Probst, A.V., Fagard, M., Proux, F., Mourrain, P., Boutet, S., Earley, K., Lawrence, R.J., Pikaard, C.S., Murfett, J., Furner, I., Vaucheret,

H., and Scheid, O.M. (2004). Arabidopsis histone deacetylase HDA6 is required for maintenance of transcriptional gene silencing and determines nuclear organization of rDNA repeats. Plant Cell **16:** 1021–1034.

Raizada, M.N., Benito, M.I., and Walbot, V. (2001). The MuDR transposon terminal inverted repeat contains a complex plant promoter directing distinct somatic and germinal programs. Plant J. **25:** 79–91.

Rossi, V., Hartings, H., and Motto, M. (1998). Identification and characterisation of an RPD3 homologoue from maize (*Zea mays* L.) that is able to complement an rpd3 null mutant of *Saccharomyces cerevisiae.* Mol. Gen. Genet. **258:** 288–296.

Rossi, V., Locatelli, S., Lanzanova, C., Boniotti, B., Varotto, S., Pipal, A., Goralik-Schramel, M., Lusser, A., Gatz, C., Gutierrez, C., and Motto, M. (2003). A maize histone deacetylase and retinoblastoma-related protein physically interact and cooperate in repressing gene transcription. Plant Mol. Biol. **51:** 401–413.

Schubeler, D., and Turner, B.M. (2005). A new map for navigating the yeast epigenome. Cell **122:** 489–492.

Shi, J., and Dawe, R.K. (2006). Partitioning of the maize epigenome by the number of methyl groups on histone H3 lysines 9 and 27. Genetics **173:** 1571–1583.

Smith, D., Greene, B., Veit, B., and Hake, S. (1992). A dominant mutation in the maize homeobox gene, Knotted-1, causes its ectopic expression in leaf cells with altered fates. Development **116:** 21–30.

Smyth, G.K. (2004). Linear models and empirical Bayes methods for assessing differential expression in microarray experiments. Stat. Appl. Genet. Mol. Biol. **3:** 1–3.

Strahl, B.D., and Allis, C.D. (2000). The language of covalent histone modifications. Nature **403:** 41–45.

Tariq, M., Saze, H., Probst, A.V., Lichota, J., Abu, Y., and Paszkowski, J. (2003). Erasure of CpG methylation in Arabidopsis alters patterns of histone H3 methylation in heterochromatin. Proc. Natl. Acad. Sci. USA **100:** 8823–8827.

Thiagalingam, S., Cheng, K.H., Lee, H.J., Mineva, N., Thiagalingam, A., and Ponte, J.F. (2003). Histone deacetylases: Unique players in shaping the epigenetic histone code. Ann. N. Y. Acad. Sci. **983:** 84–100.

Tian, L., and Chen, Z.J. (2001). Blocking histone deacetylation in Arabidopsis induces pleiotropic effects on plant gene regulation and development. Proc. Natl. Acad. Sci. USA **98:** 200–205.

Tian, L., Fong, M.P., Wang, J., Wei, N.E., Jiang, H., Doerge, R.W., and Chen, Z.J. (2005). Reversible histone acetylation and deacetylation mediate genome-wide, promoter-dependent and locus-specific changes in gene expression during plant development. Genetics **169:** 337–345.

Tian, L., Wang, J., Fong, M.P., Chen, M., Cao, H., Gelvin, S.B., and Chen, Z.J. (2003). Genetic control of developmental changes induced by disruption of Arabidopsis histone deacetylase 1 (*AtHD1*) expression. Genetics **159:** 399–409.

Timmermans, M.C., Hudson, A., Becraft, P.W., and Nelson, T. (1999). ROUGH SHEATH2: A Myb protein that represses knox homeobox genes in maize lateral organ primordia. Nature **284:** 151–153.

Tsiantis, M., Schneeberger, R., Golz, J.F., Freeling, M., and Langdale, J.A. (1999). The maize rough sheath2 gene and leaf development programs in monocot and dicot plants. Nature **284:** 154–155.

Turner, B.M. (2005). Reading signals on the nucleosome with a new nomenclature for modified histones. Nat. Struct. Mol. Biol. **12:** 110–112.

Varotto, S., Locatelli, S., Canova, S., Pipal, A., Motto, M., and Rossi, V. (2003). Expression profile and cellular localization of maize Rpd3-type histone deacetylases during plant development. Plant Physiol. **133:** 606–617.

Walsh, J., and Freeling, M. (1999). The liguleless2 gene of maize functions during the transition from the vegetative to the reproductive shoot apex. Plant J. **19:** 489–495.

Wiren, M., Silverstein, M.A., Sinha, I., Walfridsson, J., Lee, H.M., Laurenson, P., Pillus, L., Robyr, D., Grunstein, M., and Ekwal, K. (2005). Genomewide analysis of nucleosome density histone acetylation and HDAC function in fission yeast. EMBO J. **24:** 2906–2918.

Zhou, C., Zhang, L., Duan, J., Miki, B., and Wu, K. (2005). HISTONE DEACETYLASE 19 is involved in jasmonic acid and ethylene signaling of pathogen response in Arabidopsis. Plant Cell **17:** 1196–1204.